Combined Model Profile
Version: 1.0.00
Released: 2025-09-30

Bladder Cancer Combined Model Profile

Individual Model Profiles

Cancer of the Bladder R-based Analytic Simulator (COBRAS): Model Profile
University of Ottawa
Version: 1.0.00
Released: 2025-09-30

The Kystis Bladder Cancer Population Model: Model Profile
Brown University
Version: 1.0.00
Released: 2025-09-30

Simulation of Cancers of the Urinary Tract (SCOUT): Model Profile
Columbia University Irving Medical Center
Version: 1.0.00
Released: 2025-09-30

Suggested citation

CISNET Bladder Working Group. Bladder Cancer Combined Model Profile. [Internet] Sep 30, 2025. Cancer Intervention and Surveillance Modeling Network (CISNET). Available from: https://cisnet.cancer.gov/resources/files/mpd/bladder/CISNET-bladder-combined-model-profile-1.0.00-2025-09-30.pdf

Combined Model Profile Version Table

Version	Date	Notes
1.0.00	2025-09-30	Initial release

University of Ottawa
Version: 1.0.00
Released: 2025-09-30

Cancer of the Bladder R-based Analytic Simulator (COBRAS): Model Profile

University of Ottawa

Contact

Hawre Jalal (hjalal@uottawa.ca)

Funding

The development of this model was supported by the NIH/NCI CISNET Bladder Cancer Grant (U01CA265750).

Suggested Citation

Garibay-Trevino DU, Alarid-Escudero F, Kumar P, Jacobs B, Chowdhury KR, Chiddarwar T, Osei P, Kuntz K, Jalal H. Cancer of the Bladder R-based Analytic Simulator (COBRAS): Model Profile. [Internet] Sep 30, 2025. Cancer Intervention and Surveillance Modeling Network (CISNET). Available from: https://cisnet.cancer.gov/resources/files/mpd/bladder/CISNET-bladder-cobras-model-profile-1.0.00-2025-09-30.pdf

Version Table

Version	Date	Notes
1.0.00	2025-09-30	Initial release

University of Ottawa
Readers Guide

uOttawa

Reader's Guide

Core Profile Documentation

These topics will provide an overview of the model without the burden of detail. Each can be read in about 5-10 minutes. Each contains links to more detailed information if required.

Model Purpose
This document describes the primary purpose of the model.

Model Overview
This document describes the primary aims and general purposes of this modeling effort.

Assumption Overview
An overview of the basic assumptions inherent in this model.

Parameter Overview
Describes the basic parameter set used to inform the model, more detailed information is available for each specific parameter.

Component Overview
A description of the basic computational building blocks (components) of the model.

Output Overview
Definitions and methodologies for the basic model outputs.

Results Overview
A guide to the results obtained from the model.

Validation Overview
A guide to the model validation.

Key References
A list of references used in the development of the model.

uOttawa

Model Purpose

Summary

The Cancer of Bladder R Analytic Simulator (COBRAS) is an individual-level discrete event simulation (DES) model designed to simulate the onset, progression, detection, recurrence, and treatment of bladder cancer in the U.S. population. The model was developed to provide insights into, and inform optimal health policy strategies for, reducing the incidence and mortality of bladder cancer.

Purpose

COBRAS is intended as a tool to assess bladder cancer development, as well as the costs and outcomes associated with various interventions aimed at lowering bladder cancer incidence and mortality in the United States. These interventions can include new screening regimens and the adoption of emerging detection tests.

The model's key aims are:

1. Estimate natural history parameters that govern bladder cancer development in a simulated population.
2. Quantify disease burden under changing demographic conditions, such as an aging population.
3. Evaluate the effectiveness, costs, and cost-effectiveness of a range of health strategies, including screening, surveillance, and treatment.

By integrating data on disease progression, screening performance, and treatment outcomes, COBRAS can help guide decisions about how best to allocate resources and implement policies that diminish the burden of bladder cancer in the United States.

University of Ottawa
Model Overview

uOttawa

Model Overview

Summary

This section provides an overview of the COBRAS model's structure and its major components.

Purpose

The COBRAS model was developed to evaluate different screening and surveillance programs by comparing the cost, effectiveness, and cost-effectiveness of various bladder cancer detection and treatment strategies. To achieve this, COBRAS simulates the natural history of bladder cancer in the U.S. population and calibrates its underlying disease parameters using SEER data.

By modeling how bladder cancer lesions emerge in each individual, how they progress, and how death occurs from bladder or other causes, the COBRAS model provides insights into the potential impact of alternative policies aimed at reducing bladder cancer incidence and mortality.

Background

Bladder cancer predominantly affects older adults, with nine out of ten cases occurring in individuals older than 55 years of age, and the average age at detection being 73 [1]. Men experience bladder cancer at a rate four times higher than women [1]. Additionally, White men have twice the incidence compared with Black, Hispanic, or Asian/Pacific Islander men [1]. It remains uncertain whether these differences stem from variation in risk exposures, biological factors, or disparities in access to medical care.

Model Description

The COBRAS model is an individual-level discrete event simulation (DES) framework that generates a U.S. synthetic population and projects bladder cancer incidence and mortality. It is implemented in the R programming language [2].

Each simulated individual is assigned race, sex, and birth year, along with a time of death from causes other than bladder cancer. The model also determines who develops lesions, how many they develop, and each lesion's initial stage at onset. Based on this information, COBRAS simulates the time to death from bladder cancer using a fast vectorized algorithm [3].

The baseline version of COBRAS generates birth cohorts from 1900 onward, combining them up to create a population snapshot in the calendar year 2010 for analysis. This can be adapted to simulate cohorts up to 2060 or other time horizons. The model comprises the following components (**Figure 1**):

- a birth cohort generator module,
- a smoking history generator,
- a background mortality module,
- a tumor generator module,
- a tumor growth module,
- a nodal involvement and distant metastasis module,
- a diagnosis module,
- a bladder cancer mortality module, and
- a post diagnosis treatment and surveillance module.

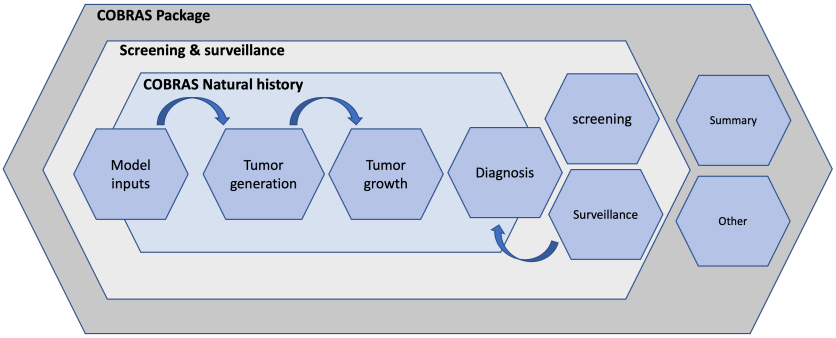

Figure 1: COBRAS model structure.

Additional details on population demographics, the natural history of bladder cancer, and the specified screening and surveillance programs appear in the Assumption Overview. The Parameter Overview describes the variables used to model natural history, screening, and surveillance.

References

1. National Cancer Institute. Surveillance, Epidemiology, and End Results Program: Cancer Stat Facts, Bladder Cancer [Internet]. 2024. Available from: https://seer.cancer.gov/statfacts/html/urinb.html/
2. R Core Team. R: A Language and Environment for Statistical Computing [Internet]. Vienna, Austria: R Foundation for Statistical Computing; 2025. Available from: https://www.R-project.org/
3. David U Garibay-Treviño, Hawre Jalal, Fernando Alarid-Escudero. A Fast Nonparametric Sampling Method for Time to Event in Individual-Level Simulation Models. Medical Decision Making. SAGE Publications Sage CA: Los Angeles, CA; 2025;0272989X241308768.

Assumption Overview

Summary

This section outlines the key assumptions of the COBRAS Model, which are informed by both scientific literature and clinician expertise.

Background

The COBRAS model rests on several fundamental assumptions regarding bladder cancer pathogenesis and progression. It is structured to be flexible for sex- and race-specific differences yet retains a uniform modeling approach for all population subgroups.

Assumption Listing

Demographic Assumptions

Background Mortality

COBRAS samples each individual's background mortality age using U.S. Life Tables. Year-, sex-, race-, and age-specific mortality probabilities are employed in a categorical distribution to determine the age of death from causes unrelated to bladder cancer.

Natural History Assumptions

Risk of Bladder Cancer

COBRAS uses a binomial process to designate which individuals develop bladder cancer:

$$BC_i \sim \text{Binomial}(P(BC_i))$$

where the probability of developing bladder cancer in the i-th individual is given by:

$$P(BC_i) = \frac{1}{1 + \exp(-\text{odds}_i)}$$

and

$$\text{odds}_i = \alpha_0 + \alpha_1 \cdot \text{sex}_i + \alpha_2 \cdot \text{race}_i + \alpha_3 \cdot \text{smoking}_i$$

- α_0 is baseline odds for white males.
- α_1 reflects the odds difference for females relative to males (sex_i = 0 for males, 1 for females).
- α_2 is the odds difference for black individuals vs. white individuals.
- α_3 is the odds difference for smokers vs. nonsmokers.

Tumor Generation

For individuals who develop bladder cancer, the number of tumors (c_i) follows a zero-truncated Poisson distribution:

$$c_i \sim \text{Trunc Poisson}(\lambda_i | a = 0)$$

with

$$\log(\lambda_i) = \beta_{0_i} + \beta_{\text{sex}} \cdot \text{sex}_i + \beta_{\text{race}} \cdot \text{race}_i + \beta_{\text{smoking}} \cdot \text{smoking}_i$$

The baseline risk (β_{0_i}) has a normal distribution:

$$\beta_{0_i} \sim \text{Normal}(\beta_0, \sigma^2_{\beta_0})$$

Age of Patient at Lesion Onset

The age of patient at lesion onset is modeled using a Weibull distribution:

$$\text{age of patient at lesion onset}_i \sim \text{Weibull}(\tau, \theta_i)$$

where the individual-specific scale (θ_i) is drawn from a lognormal distribution:

$$\theta_i \sim \text{Lognormal}(\mu_{\text{scale}}, \sigma_{\text{scale}})$$

Allowed Initial Tumor Types

Individuals may initially develop Tis, Ta low-grade (Ta-lg), or Ta high-grade (Ta-hg) tumors (see **Figure 1**). The onset tumor type is assigned via a categorical distribution:

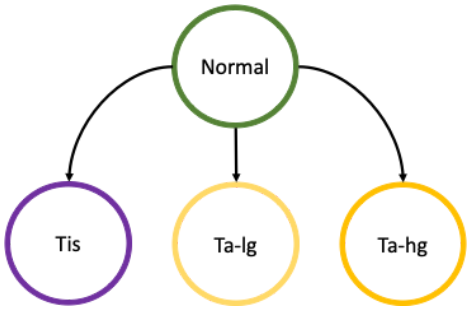

Figure 1: Allowed initial tumor types in the COBRAS model.

$$\text{type at onset} \sim \text{Categorical}(P_{\text{Tis}}, P_{\text{Ta-lg}}, P_{\text{Ta-hg}})$$

where P_{Tis} and P_{Ta-hg} are estimated from the literature, and $P_{\text{Ta-lg}} = 1 - (P_{\text{Tis}} + P_{\text{Ta-hg}})$

Possible Transitions

Once the initial tumor type is set, transitions among clinical and preclinical tumor stages occur as depicted in **Figure 2**.

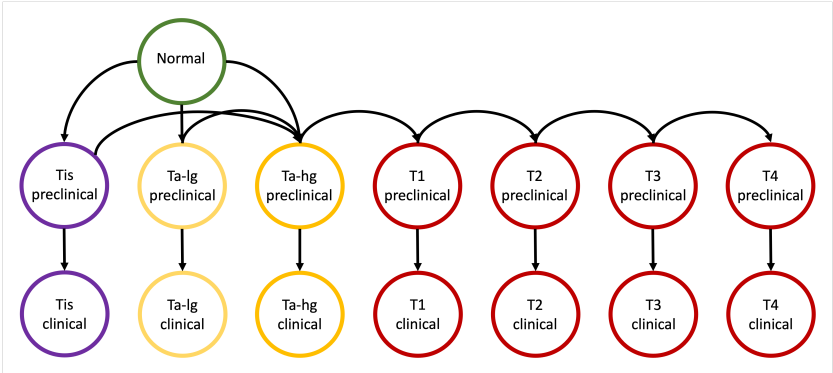

Figure 2: Allowed transitions between clinical and preclinical stages in the COBRAS model.

Tumor Growth

Tumors are classified as muscle-invasive bladder cancer (MIBC) or non-muscle-invasive bladder cancer (NMIBC). MIBC growth rates are exponential and stage-specific, while NMIBC growth follows a Gompertz model. These parameters are calibrated to SEER data.

For MIBC, we assume an exponential transition rate between tumor stages. These rates are T-stage-specific and assumed to be higher for the more advaced stages.

For individuals who develop Tis tumors, we consider a multiplicative hazard ratio applied to the MIBC growth rate. This hazard ratio was implemented considering that individuals with Tis have a different tumor development progression behavior.

For NMIBC, we assume that tumors have a spherical shape and that the tumor sizes areis defined by the diameter of the sphere. The speed of NMIBC growth is defined by a Gompertz distribution considering that all tumors have an initial size of 1 millimeter. In the model we obtain the time to arrive to the following NMIBC sizes: 0.5 centimeters (cm), 1 cm, 3 cm, 5 cm, and 8 cm. The asymptote of the Gompertz growth curve represents maximum NMIBC size, and currently has a value of 2,150 cubic centimeters, which comes from a diameter of approximately 16 cm.

Nodal Involvement and Metastasis

Lymph node involvement is modeled as a two-step process: No involvment (N0) to local involvement (N1) to distant involvement (N2). These transition rates follow exponential functions and are calibrated. Similarly, metastasis is a binary variable, with time to metastasis drawn from an exponential distribution.

Bladder Cancer Diagnosis (Detection)

MIBC tumors are detected based on stage-specific exponential rates. Detection rates for Tis, Ta-lg, Ta-hg and T1 are assumed to be unknown and are calibrated. For MIBC stages T2, T3, and T4 are derived using log hazard ratios to ensure ordinal detection rates relative to T1, such that

$$\log(r_{T_{i+1}}) = \log(r_{T_i}) + \log(\mathrm{HR}_{i+1}).$$

Competing risks are considered during detection. A tumor will be detected in a particular stage if the time to detection is lower than the transition time to the next stage.

Once a tumor is detected in an individual, we assume that this individual will have a test to detect the rest of the tumors. Currently we assume a 95% test sensitivity for all tumor types. The same test sensitivity is applied during surveillance visits.

With the information of all the detected tumors, the patient is classified for surveillance considering the most advanced detected tumor, and their metastasis and nodal involvement status of the detected tumors at symptom detection.

Bladder Cancer Mortality

Bladder cancer mortality is determined using stage-specific exponential rates driven from SEER relative risk of survival. The age of death is the minimum of the background mortality age and the bladder cancer mortality age.

Surveillance Assumptions

Surveillance Schedules

Patients are classified into risk categories based on the NCCN Clinical Practice Guidelines. Surveillance schedules are defined as follows:

- **Low Risk**: Solitary Ta-lg tumor ≤ 3 cm.
- **Intermediate Risk**: Includes solitary Ta-hg tumor ≤ 3 cm, multifocal Ta-lg, Ta-lg recurrence within a year, or Ta-lg > 3 cm.
- **High Risk**: Includes T1/CIS lesions, multifocal Ta-hg, Ta-hg recurrence within a year, or Ta-hg > 3 cm.

Surveillance schedules for each risk category are summarized in **Table 1**:

Table 1. Surveillance schedules by risk category

A. Low-risk patients

Years	Months
1	3 & 12
2 to 5	Annually

Years	Months
10+	As clinically indicated

B. Intermediate-risk patients

Years	Months
1	3, 6 & 12
2	Every 6 months
3 to 5	Annually
5+	As clinically indicated

C. High-risk patients

Years	Months
1 to 2	Every 3 months
3 to 5	Every 6 months
5 to 10	Annually
10+	As clinically indicated

During each surveillance visit, the following steps are performed:

1. Confirm the patient is alive.
2. Verify attendance at the appointment.
3. Check for undetected tumors.
4. Detect any new tumors and redefine the patient's classification if necessary.

These steps are summarized in **Figure 3**.

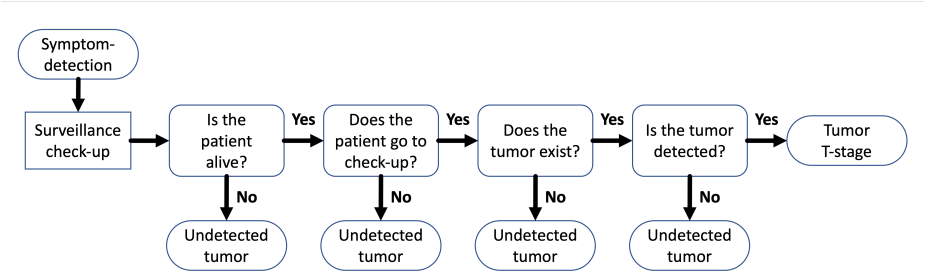

Figure 3: Surveillance flowchart.

The probability of attending a surveillance visit and detecting new tumors is modeled using binomial distributions. Test sensitivity remains consistent with the natural history module.

uOttawa

Parameter Overview

Summary

This document provides an overview of the demographic and natural history parameters used in the COBRAS model.

Background

TCOBRAS integrates two major parameter sets: demographic parameters (which specify characteristics of a simulated population, such as race, sex, and mortality) and natural history parameters (which govern how bladder cancer develops and progresses). Some of these natural history parameters also affect other processes, such as tumor detection during surveillance.

Parameter Listing Overview

Population demographics

COBRAS assigns each simulated individual a birth year, race, sex, smoking status, and an age of death due to causes other than bladder cancer. These demographic variables reflect U.S. population trends and are based on published life tables [1]. Each individual is assumed to have a single outcome for background mortality (i.e., an age of death unrelated to bladder cancer).

Currently, COBRAS includes only two race categories (Black and White) and two sex categories (male and female). Future expansions may incorporate additional categories. Smoking status is binary (smoker vs. non-smoker) and is currently set to “non-smoker” in the baseline version. Population size, as well as the distribution of sex and race, are calibrated against empirical data.

Natural history parameters

All of COBRAS’s natural history parameters fall into several conceptual areas:

1. **Risk of Developing Bladder Cancer**
   Each individual has a probability of developing bladder cancer that reflects demographic differences (e.g., sex, race) and possible behavioral factors such as smoking.

2. **Number of Tumors**
   Once an individual is designated to develop bladder cancer, the model determines how many tumors appear. This number can vary due to differences in baseline risk across the population.

3. **Age at Lesion Onset**
   The time at which bladder lesions appear follows a distribution that allows for variability among individuals. COBRAS can incorporate both group-level differences (such as sex or race) and person-level random variation.

4. **Initial Tumor Types**
   When a tumor is first created, it may present as one of several possible stages, such as Ta (low- or high-grade) or Tis. The probability of each initial stage is determined by empirical data.

5. **Tumor Progression**

   - **Muscle-Invasive Bladder Cancer (MIBC)**: Progresses through clinical stages via exponential transitions. A hazard ratio can be applied to certain subgroups (e.g., Tis) to capture faster or slower progression.
   - **Non–Muscle-Invasive Bladder Cancer (NMIBC)**: Uses a growth curve to capture changes in tumor volume over time.

6. **Nodal Involvement and Metastasis**
   Time to lymph node involvement (N1, N2) and time to distant metastasis are each modeled with exponential rates.

7. **Detection by Symptoms**
   Symptomatic detection occurs when a tumor has progressed sufficiently to cause clinical signs. Different stages (T1, T2, T3, T4) may have different detection rates.

8. **Test Sensitivity**
   When the model simulates a clinical exam (for example, during screening or surveillance), detection probabilities vary by tumor stage, reflecting differences in test performance.

9. **Bladder Cancer Mortality**
   The model applies stage-specific mortality rates to each tumor type. Individuals may die from bladder cancer or from other causes, whichever occurs first.

Surveillance parameters

During surveillance, patients will have appointments to be checked for new tumors. The surveillance schedule inside the COBRAS model has been defined by following the The model includes three levels of patient risk during surveillance: low, intermediate and high risk. The risk-specific schedules are defined by the following parameters:

Following detection or diagnosis, patients enter a surveillance schedule. COBRAS adapts the NCCN Clinical Practice Guidelines schedules[2] with risk-based screening intervals for follow-up:

- **Low risk:** Follow-ups at longer intervals.
- **Intermediate risk:** More frequent follow-ups than low risk.
- **High risk:** The most frequent follow-up schedule.

At each visit, a patient has a certain probability of attending (adherence), and any new or progressing tumor may be detected according to the same stage-specific test sensitivities. If newly detected lesions are found, the patient's risk category—and thus their follow-up schedule—can change accordingly.

Calibrated parameters

COBRAS includes both calibrated and fixed parameters:

- **Calibrated parameters** are estimated by matching model outputs to population-level data (e.g., SEER). These include the parameters governing tumor progression rates and the symptomatic detection process.
- **Fixed parameters** use direct estimates from literature or expert consensus. Examples include certain baseline mortality rates and default test sensitivities.

An example of a calibrated parameter is the transition rate from Tis to T1, which is estimated via calibration. An example of a fixed parameter is the maximum tumor volume assumed for NMIBC growth.

Table 1 provides a high-level look at the main parameters, indicating which ones are calibrated or fixed, as well as their plausible ranges or baseline values. (See the full table for specific numerical bounds.)

Table 1. Calibrated parameters in the COBRAS model

Parameter Group	Example Variables	Calibrated?	Notes
BC Risk & Incidence	Sex/race differences, smoking status	Yes	Key driver of who develops cancer
Tumor Generation	Number of tumors, initial stage probabilities	Yes	Zero-truncated Poisson approach

Parameter Group	Example Variables	Calibrated ?	Notes
Age of Onset	Distribution shape/scale for lesion onset	Yes	Uses Weibull or log-normal combo
Progression Rates	MIBC stage transitions, NMIBC growth parameters	Yes	Typically exponential or Gompertz
Detection Rates	Stage-specific detection by symptoms or tests	Yes	Calibrated to reflect real-world
Mortality Rates	Stage-specific hazard of BC death	No	Often derived from SEER data
Surveillance	Schedule intervals, adherence probability	No	Based on guidelines & assumptions

References

1. Elizabeth Arias, Jiaquan Xu, Kenneth Kochanek. United States life tables, 2021. 2023;
2. National Comprehensive Cancer Network, others. NCCN clinical practice guidelines in oncology. http://www nccn org/professionals/physician_gls/PDF/occult pdf. 2008;

University of Ottawa
Component Overview

uOttawa

Component Overview

Summary

This section describes the major components of the COBRAS model, illustrating how each module interacts to simulate the development, detection, and outcomes of bladder cancer at the population level.

Overview

COBRAS simulates a population of individuals (by age, sex, race, and smoking history), follows them over time, and projects the incidence and mortality of bladder cancer. COBRAS is a population model, meaning it starts simulating each birth-year cohort starting in 1900. The outcomes in each calendar year is created by combining outcomes for the cohorts that contribute to the U.S. population composition in that year. For example, the population outcome for the calendar year 2010 involves birth-year cohorts born between 1910 and 2010.

COBRAS uses a series of interconnected modules, each responsible for a key aspect of disease progression, detection, and patient follow-up. The overall structure is presented in **Figure 1**.

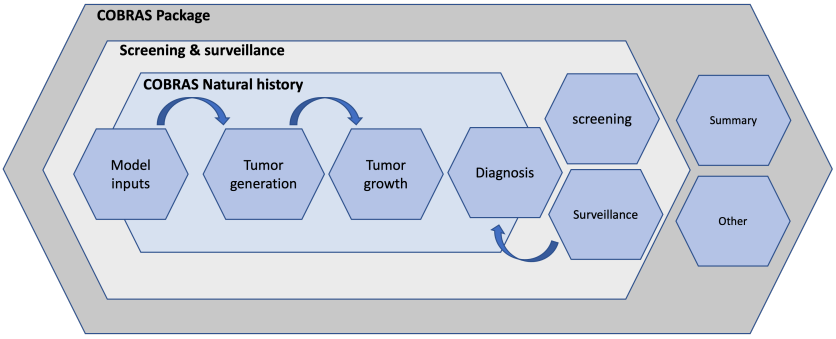

Figure 1: COBRAS model structure.

Currently, COBRAS includes the following components:

- A **population generator** to create a synthetic cohort including their history of smoking
- A **bladder cancer natural history** module
- A **mortality** module
- A **surveillance** module
- A **summary** module of key results

A **screening** module is planned for future development.

Component Listing

Population generator

The population generator produces a synthetic cohort that reflects demographic characteristics (race, sex, birth year) and smoking histories. It also assigns a background mortality age for each individual based on external life table data. Individuals are then followed in the simulation according to their demographic traits and mortality risk. In addition, smoking history for each individual is obtained from the Smoking History Generator.

Bladder Cancer natural history

The natural history module determines:

1. **Who develops bladder cancer** among the simulated population.
2. **How many tumors** each affected individual generates.
3. **Tumor characteristics**, including initial stage (e.g., Tis, Ta-low-grade, Ta-high-grade), growth patterns (muscle-invasive vs. non–muscle-invasive), and potential transitions to more advanced stages.

- **Muscle-invasive growth** is assumed stage-specific and can involve hazard ratios for tumors originating as Tis.
- **Non–muscle-invasive growth** follows a Gompertz-like curve, treating tumors as spherical until they reach a pre-defined maximum size.
- **Nodal involvement and metastasis** are allowed for tumors that start at Tis or Ta-high-grade, though these do not currently alter mortality rates or other natural history processes beyond their point of detection.

The module simulates **symptomatic detection** using stage-specific detection rates. If a tumor is detected, the individual undergoes an evaluation that can identify additional tumors. Detection triggers a risk classification process based on guidelines [1], and the individual's time to death from bladder cancer is set, using stage-specific mortality rates starting from the time of detection.

Mortality module

This module integrates:

- **Background mortality** from U.S. Life Tables (e.g., from heart disease or other causes).
- **Bladder cancer mortality** (time from symptomatic detection to death).

Each individual's final age of death is the minimum of these two ages. If an individual never develops bladder cancer, their cause of death is attributed to non-bladder causes.

Surveillance module

Once a tumor is detected, the individual enters a surveillance schedule with periodic checkups. The frequency of these visits depends on the patient's risk category at the time of detection. During each surveillance visit:

1. The individual may or may not attend (based on an adherence probability).
2. Additional tumors can be detected, potentially changing the patient's risk classification.
3. Surveillance continues until either the scheduled visits are completed or the patient dies.

Screening module

A formal screening module has not yet been implemented. Future releases of COBRAS will incorporate population-based screening strategies, enabling comparisons of different screening intervals and test modalities.

Summary module

Finally, COBRAS aggregates model outputs to facilitate validation and policy analysis. Key outcomes include:

- **Age-specific incidence rates**
- **Stage-specific incidence rates**
- **Proportion of tumors by stage**
- **Lifetime risk of bladder cancer**
- **Age of tumor onset and symptomatic detection**
- **Sojourn time** (the interval from tumor onset to its symptomatic detection)

These outputs are stratified by sex and race, providing insights into the epidemiology of bladder cancer in the simulated population.

References

1. National Comprehensive Cancer Network, others. NCCN clinical practice guidelines in oncology. http://www nccn org/professionals/physician_gls/PDF/occult pdf. 2008;

Output Overview

Summary

This document describes the primary outputs of the COBRAS model and explains how they are defined and calculated.

Overview

COBRAS tracks each synthetic individual's life history, from birth until death for each birth-year cohort born between 1910 and 2020. In addition, the model can forecast bladder cancer outcomes through 2060 using U.S. Census projections. For those who develop bladder cancer, the model records the timing of tumor onset and detection. At the end of each simulation run, COBRAS produces a dataset representing the full natural history of bladder cancer for every simulated individual. By analyzing and summarizing these data, the model calculates its principal outputs.

Output Listing

The COBRAS model's main outputs include:

- **Age-specific incidence rate**
- **Stage-specific incidence rate**
- **Tumor proportion by stage**
- **Overall incidence**
- **Lifetime risk of developing bladder cancer**
- **Age of tumor onset**
- **Age of detection by symptoms**
- **Sojourn time**

All of these outputs can be stratified by age, sex, race, or smoking status to allow detailed analyses of subgroup differences.

Output definitions

Age-specific incidence rate

Let $ C_a $ denote the number of individuals newly diagnosed with bladder cancer in age group $ a $, and $ N_a $ the number of individuals in that same age group who are alive. The age-specific incidence rate per 100,000 persons is:

$$CI_a = 100{,}000 \times \frac{C_a}{N_a}$$

Stage-specific incidence rates

Let $ C_s $ denote the number of individuals newly diagnosed at stage $ s $, and let $ N $ represent the total living population. The incidence rate per 100,000 persons for stage $ s $ is:

$$CI_s = 100{,}000 \times \frac{C_s}{N}$$

Tumor proportion by stage

Let $ C $ be the total number of newly diagnosed cancer cases across all stages. The proportion of diagnoses occurring at stage $ s $ is:

$$P_s = \frac{C_s}{C}$$

Overall incidence

The overall incidence rate per 100,000 persons is:

$$CI = 100{,}000 \times \frac{C}{N}$$

Lifetime risk of developing bladder cancer

This metric reflects the proportion of individuals in the population who will eventually be diagnosed with bladder cancer. Let $ Surv_a $ be the proportion of the original cohort who survive to age $ a $. Then the lifetime risk of diagnosis is:

$$LR = \sum_{a=0}^{120} \Big(Surv_a \times CI_a \Big)$$

Here, $ CI_a $ is the incidence rate for age group $ a $.

Age of tumor onset

This output is the age at which tumors begin to develop in individuals who are ultimately diagnosed with bladder cancer. It focuses on the specific lesion that leads to symptomatic detection.

Age of detection by symptoms

This is the age at which bladder cancer is initially detected by symptoms during an individual's lifetime. If multiple tumors appear, only the one leading to symptomatic detection is counted in the model's records.

Sojourn time

Let $ Onset_i $ denote the tumor onset age and $ Detection_i $ the age of detection for individual $ i $. The sojourn time is:

$$Sojourn_i = Detection_i - Onset_i$$

This reflects the duration between the biological start of a tumor and the point of diagnosis through symptoms.

Results Overview

Summary

This section describes the main results generated by the COBRAS model, including key outcomes from its Bayesian calibration process and the additional model-based metrics used to validate and interpret bladder cancer incidence patterns.

Overview

The results presented here reflect the current version of COBRAS, calibrated using the BayCANN approach (see Validation Overview for details). Future versions will expand on these findings, including long-term population trends and comparisons of various health strategies to reduce bladder cancer burden.

Results Listing

1. Metamodel Fit

The COBRAS model employs an ANN (artificial neural network) metamodel to approximate its more complex natural history processes. This ANN is trained to replicate age-specific and stage-specific incidences generated by the full simulation:

- **Figure 1** compares ANN-predicted vs. model-predicted age-specific incidences.
- **Figure 2** compares ANN-predicted vs. model-predicted stage-specific incidences.

These plots illustrate how well the metamodel approximates the outputs of the original simulation.

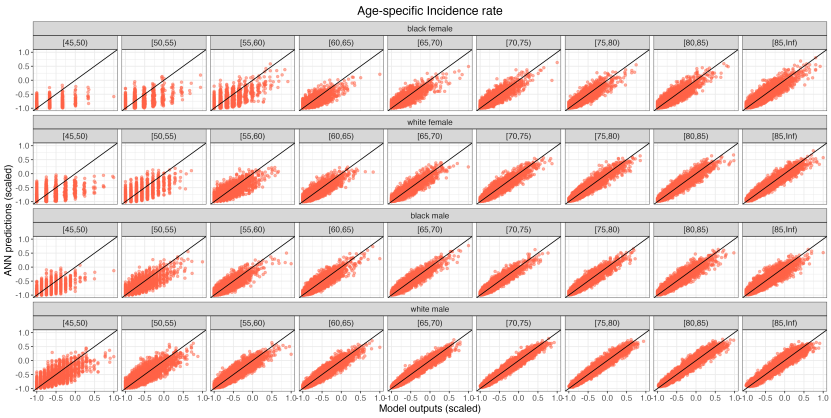

Figure 1: ANN predicted vs. model predicted age-specific incidences.

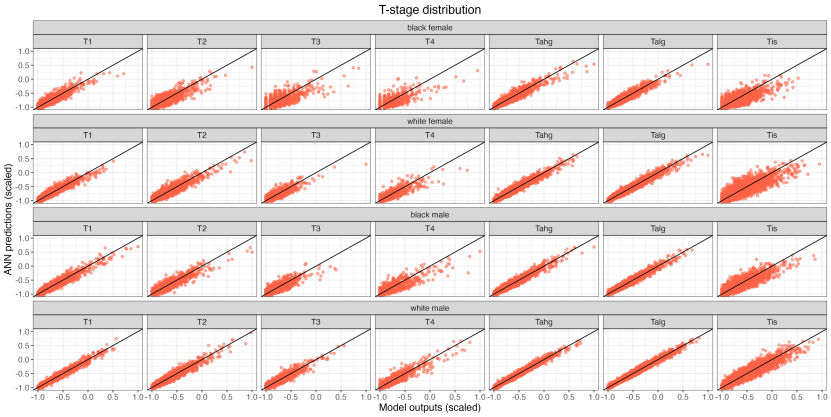

Figure 2: ANN predicted vs. model predicted stage-specific incidences.

2. Posterior Distributions of Calibrated Parameters

After training the ANN metamodel, COBRAS applies Bayesian calibration to estimate posterior distributions. The shift from prior assumptions to posterior estimates indicates how much the data inform each parameter:

Figure 3 shows prior vs. posterior distributions for the major calibrated parameters.

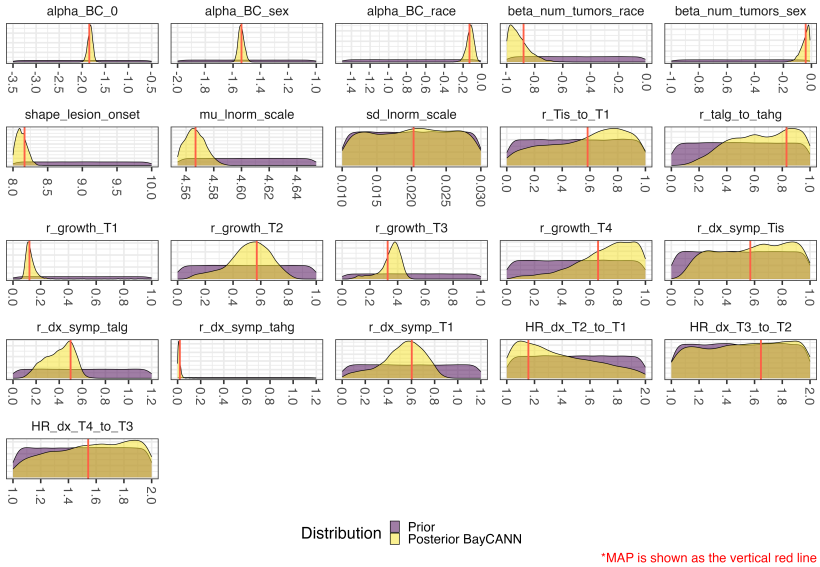

Figure 3: Prior and posterior distributions of calibrated parameters.

3. Model Validation

Using the calibrated parameter sets, COBRAS reruns the original natural history model and compares outputs with calibration targets:

- **Figure 4** presents age-specific incidence rates predicted by COBRAS relative to target data.
- **Figure 5** presents stage-specific incidence rates predicted by COBRAS relative to target data.

These comparisons help evaluate the accuracy of COBRAS in reproducing observed bladder cancer trends.

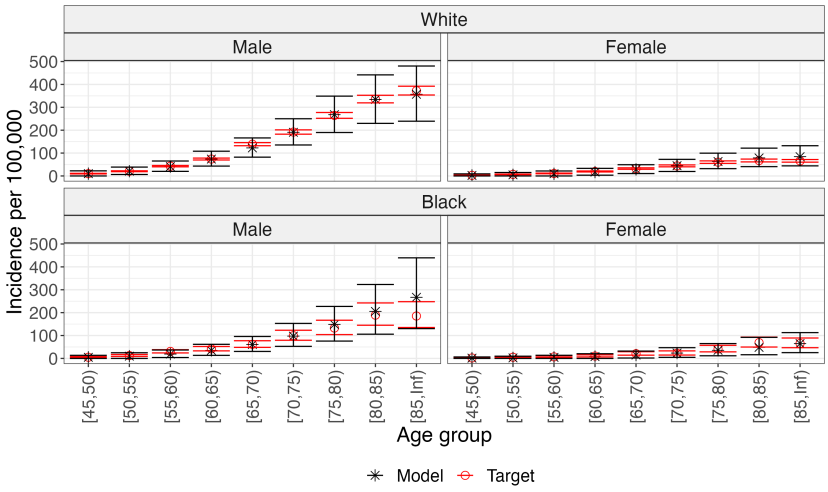

Figure 4: Age-specific incidence rates.

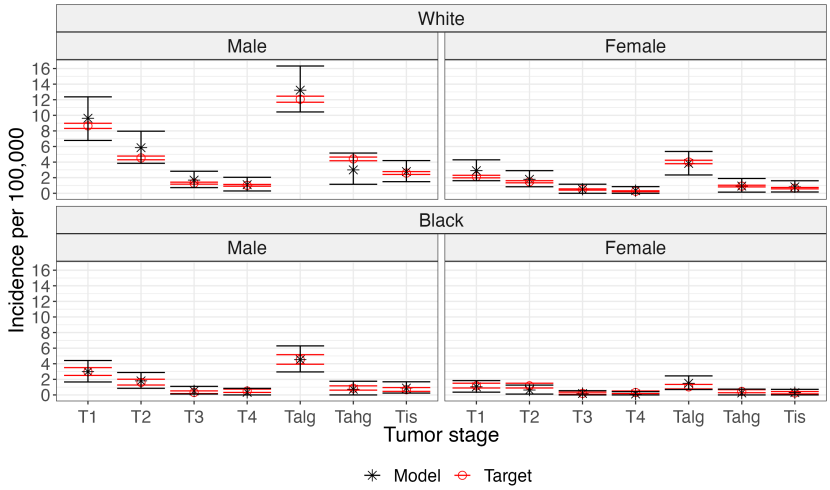

Figure 5: Stage-specific incidence rates.

4. Additional Model Outputs

Beyond the primary calibration targets, COBRAS generates a variety of supplementary results:

- **Tumor proportion by stage** (Figure 6)
- **Overall incidence** (Figure 7)
- **Lifetime risk of developing bladder cancer** (Figure 8)
- **Age of tumor onset** (Figure 9)
- **Age of symptom detection** (Figure 10)
- **Sojourn time** (Figure 11)

Each figure provides a deeper look into the natural history of bladder cancer in the simulated population.

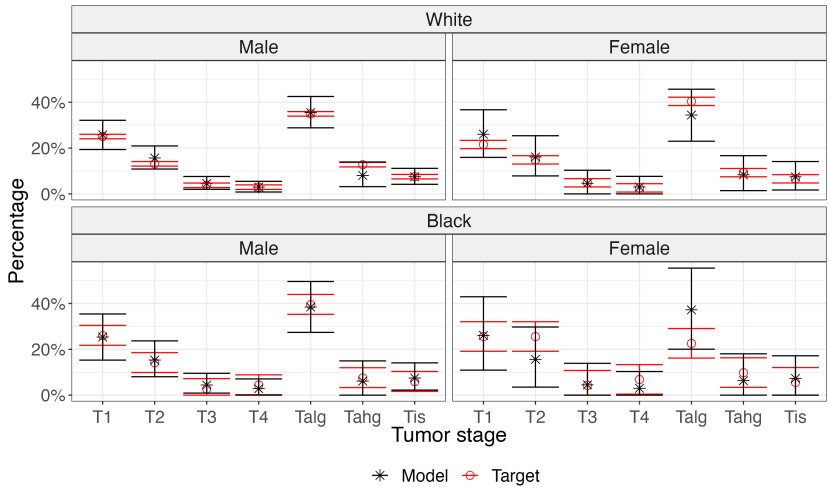

Figure 6: Tumor proportion by stage.

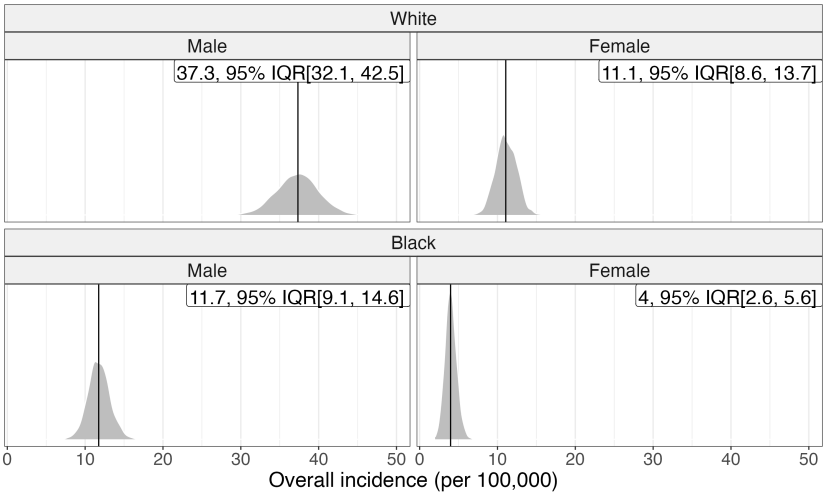

Figure 7: Overall incidence distribution.

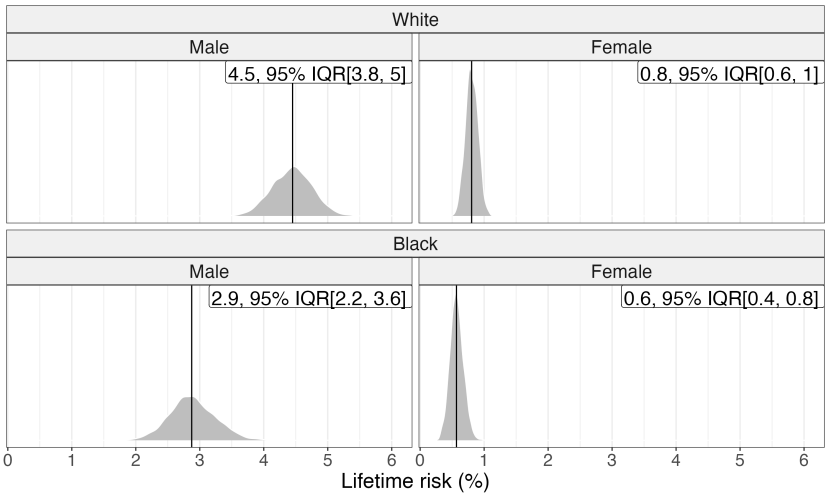

Figure 8: Lifetime risk of developing bladder cancer.

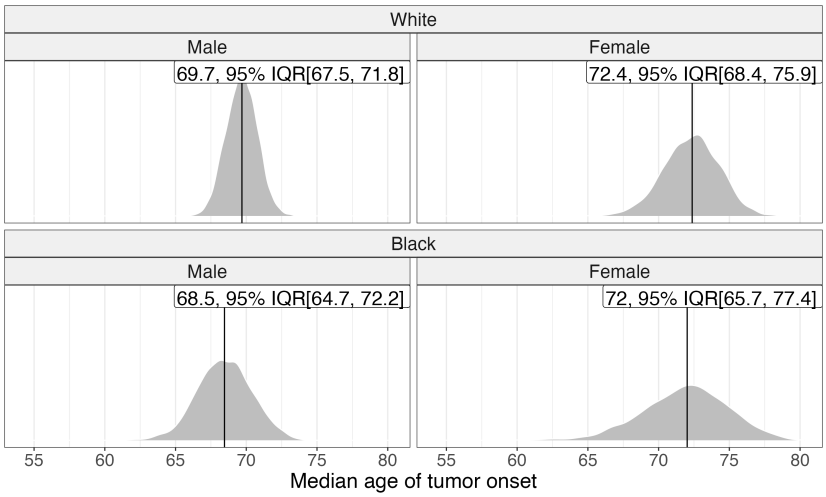

Figure 9: Age of tumor onset.

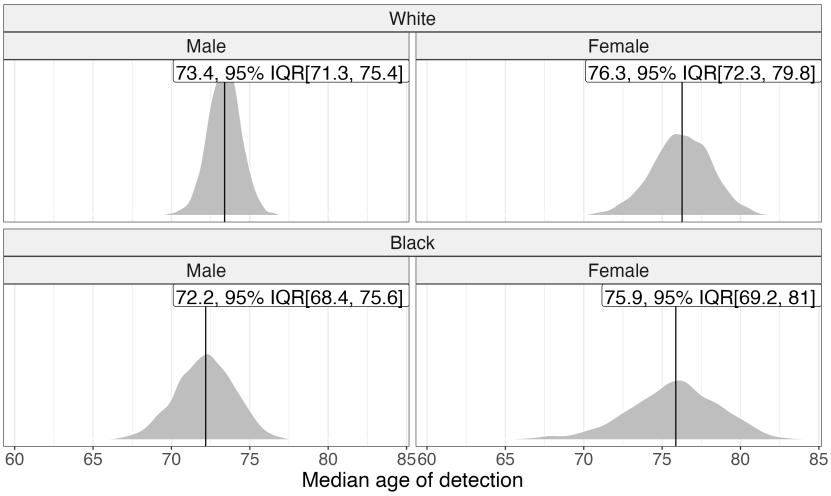

Figure 10: Age of symptom detection.

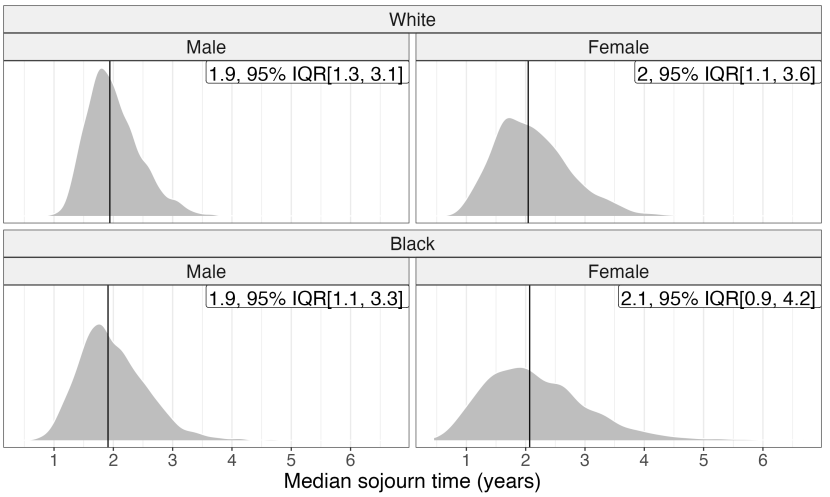

Figure 11: Median sojourn time.

University of Ottawa
Validation Overview

uOttawa

Validation Overview

Summary

This document summarizes the calibration and validation processes undertaken during the development of the COBRAS model.

Overview

COBRAS uses age- and stage-specific incidence data from 2010 Surveillance, Epidemiology, and End Results Program (SEER) statistics as primary calibration targets, stratified by sex and race for the U.S. population. To align model outputs with these targets, COBRAS employs a Bayesian Calibration using Neural Networks (BayCANN) methodology [1].

Target Definition

Age-specific incidence rates

Age-specific incidence rates for bladder cancer are computed by dividing the total number of cancer diagnoses in a given age group by the number of people alive in that age group (see the Output Overview for calculation details). COBRAS follows SEER's approach to categorizing age groups (0, 1–4, 5–9, …, 85+) but focuses on ages 45–49 and older for calibration. Rates are reported per 100,000 individuals, disaggregated by sex and race, with 95% confidence intervals constructed under a Poisson distribution assumption [2].

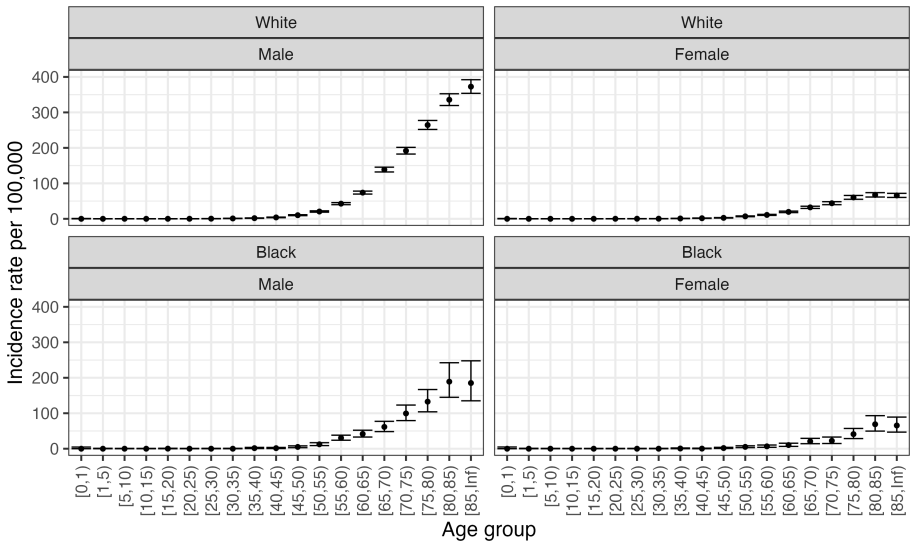

Figure 1: Age-specific incidence rate targets in the COBRAS model.

Stage-specific incidence rates (per 100,000)

Stage-specific incidence rates are computed by dividing the number of bladder cancer diagnoses at a particular stage by the number of people alive in the population. COBRAS considers the following stages: Tis, Ta–lg, Ta–hg, T1, T2, T3, and T4. These rates are stratified by sex, race, and smoking status, with 95% confidence intervals constructed similarly to the age-specific rates.

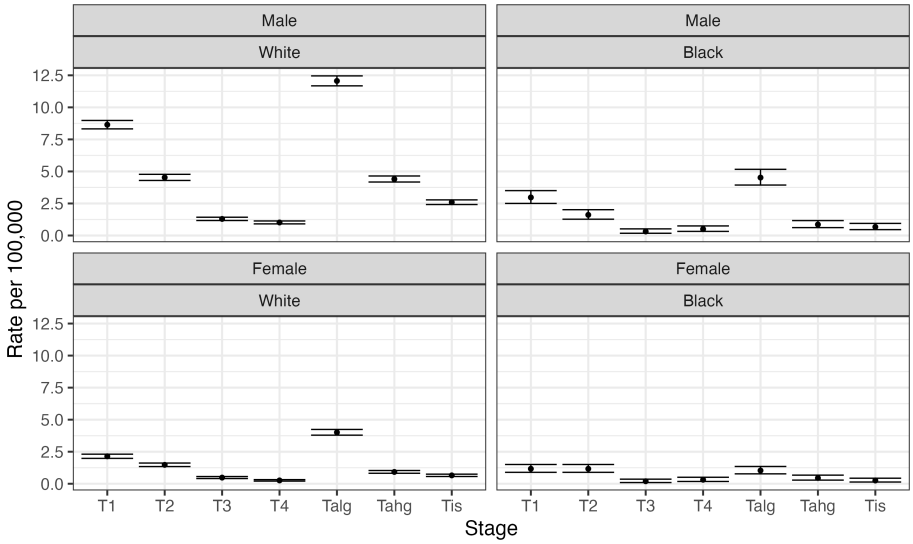

Figure 2: Stage-specific incidence rate targets in the COBRAS model.

Calibration Methodology

COBRAS relies on Bayesian Calibration using Artificial Neural Networks (BayCANN) [1] to align its outputs with target incidence data. A Bayesian approach estimates the full joint posterior distribution of parameters, capturing uncertainty more comprehensively. The BayCANN procedure consists of:

1. **Parameter Sampling**
   A set of plausible parameter values is generated using Latin Hypercube Sampling (LHS), defining lower and upper bounds for each calibrated parameter to ensure consistent sampling.

2. **Metamodel Training**
   An artificial neural network (ANN) is trained on the parameter sets and their corresponding model outputs, acting as a metamodel that can quickly approximate COBRAS output.

3. **Bayesian Calibration**
   A probabilistic programming environment is used to calibrate the ANN metamodel to observed data, treating the sampled parameters as an initial (prior) distribution.

4. **Posterior Distribution**
   Once the ANN is calibrated, it produces a posterior distribution for each parameter, which COBRAS can then use to generate updated outputs. These outputs are compared against the original targets to assess model fit.

All COBRAS parameters—calibrated or fixed—are listed in Parameter Overview, which also specifies those currently subject to calibration. The results of this calibration appear in the Results Overview.

References

1. Hawre Jalal, Thomas A Trikalinos, Fernando Alarid-Escudero. BayCANN: streamlining Bayesian calibration with artificial neural network metamodeling. Frontiers in Physiology. Frontiers Media SA; 2021;12:662314.
2. Michael P Fay. Approximate confidence intervals for rate ratios from directly standardized rates with sparse data. Communications in Statistics-Theory and Methods. Taylor & Francis; 1999;28(9):2141–2160.

uOttawa

Key References

Elizabeth Arias, Jiaquan Xu, Kenneth Kochanek. United States life tables, 2021. 2023;

Michael P Fay. Approximate confidence intervals for rate ratios from directly standardized rates with sparse data. Communications in Statistics-Theory and Methods. Taylor & Francis; 1999;28(9):2141–2160.

David U Garibay-Treviño, Hawre Jalal, Fernando Alarid-Escudero. A Fast Nonparametric Sampling Method for Time to Event in Individual-Level Simulation Models. Medical Decision Making. SAGE Publications Sage CA: Los Angeles, CA; 2025;0272989X241308768.

Hawre Jalal, Thomas A Trikalinos, Fernando Alarid-Escudero. BayCANN: streamlining Bayesian calibration with artificial neural network metamodeling. Frontiers in Physiology. Frontiers Media SA; 2021;12:662314.

National Cancer Institute. Surveillance, Epidemiology, and End Results Program: Cancer Stat Facts, Bladder Cancer [Internet]. 2024. Available from: https://seer.cancer.gov/statfacts/html/urinb.html/

National Comprehensive Cancer Network, others. NCCN clinical practice guidelines in oncology. http://www nccn org/professionals/physician_gls/PDF/occult pdf. 2008;

R Core Team. R: A Language and Environment for Statistical Computing [Internet]. Vienna, Austria: R Foundation for Statistical Computing; 2025. Available from: https://www.R-project.org/

Brown University
Version: 1.0.00
Released: 2025-09-30

The Kystis Bladder Cancer Population Model: Model Profile

Brown University

Contact

Thomas A. Trikalinos (thomas_trikalinos@brown.edu)

Funding

The development of this model was supported by the NIH/NCI CISNET Bladder Cancer Grant (U01CA265750).

Suggested Citation

Trikalinos T, Sereda Y, Popp JH, Chrysanthopoulou SA, Huang AW, Wong JB. The Kystis Bladder Cancer Population Model: Model Profile. [Internet] Sep 30, 2025. Cancer Intervention and Surveillance Modeling Network (CISNET). Available from: https://cisnet.cancer.gov/resources/files/mpd/bladder/CISNET-bladder-kystis-model-profile-1.0.00-2025-09-30.pdf

Version Table

Version	Date	Notes
1.0.00	2025-09-30	Initial release

Brown University
Readers Guide

BROWN

Reader's Guide

Core Profile Documentation

These topics will provide an overview of the model without the burden of detail. Each can be read in about 5-10 minutes. Each contains links to more detailed information if required.

Model Purpose
This document describes the primary purpose of the model.

Model Overview
This document describes the primary aims and general purposes of this modeling effort.

Assumption Overview
An overview of the basic assumptions inherent in this model.

Parameter Overview
Describes the basic parameter set used to inform the model, more detailed information is available for each specific parameter.

Component Overview
A description of the basic computational building blocks (components) of the model.

Output Overview
Definitions and methodologies for the basic model outputs.

Results Overview
A guide to the results obtained from the model.

Key References
A list of references used in the development of the model.

Model Purpose

Summary

Kystis is a discrete event microsimulation model of bladder cancer in the U.S. population. It simulates individuals who, depending on their demographic characteristics and exposure history, may develop bladder lesions throughout their lives. The model simulates bladder cancer's natural history, including symptom development and disease progression, clinical detection, treatment, and mortality. It was developed to assess bladder cancer prevention, detection, and management strategies at both population and individual levels.

Purpose

Kystis was developed to analyze bladder cancer trends and evaluate the impact of interventions, such as targeted screening, surveillance strategies for non-muscle invasive bladder cancer, and treatments for organ-confined bladder cancer.

Kystis aims to address the following questions:

- **Impact of carcinogens on past bladder cancer outcomes**. Smoking accounts for approximately 50% of all bladder cancer cases in men and up to 30% in women.[1-3]Despite decreases in smoking and various environmental exposure regulations, the incidence of bladder cancer has remained relatively stable over the past five decades, unlike the declining trends seen in other smoking-related cancers, such as lung cancer.[4,5] Our model aims to provide explanations for this discrepancy.
- **Population impact of widespread implementation of carcinogen control policies on bladder cancer prevention**. We will estimate the impact of existing policies that reduce smoking and/or other relevant carcinogens on the prevention of bladder cancer.
- **Effectiveness of bladder cancer screening among high-risk subgroups**. Routine bladder cancer screening is not recommended in the U.S. in part because of low disease incidence and the invasive nature of cystoscopy.[6] We will examine feasible screening strategies for high-risk subgroups, defined by combinations of screening modalities and schedules.
- **Effectiveness and cost-effectiveness of risk-based surveillance strategies for patients with non-muscle invasive bladder cancer (NMIBC)**. Although NMIBC is not life-threatening, it often recurs or progresses, requiring chronic surveillance. To identify optimal strategies, we will explore feasible surveillance policies, defined by combinations of testing modalities and schedules.
- **Comparative effectiveness of treatments for organ-confined bladder cancer**. We will compare (i) intravesical treatments for NMIBC, including bacille Calmette-Guerin (BCG) immunotherapy and chemotherapies; (ii) novel treatments such as gene therapies and antibody-drug conjugates for BCG-unresponsive NMIBC; and (iii) expanding bladder-sparing options, like immune checkpoint inhibitor-based immunotherapy, to novel bladder-preserving strategies and biomarker-driven chemotherapies for muscle-invasive bladder cancer (MIBC).

References

1. Maximilian Burger, James WF Catto, Guido Dalbagni, H Barton Grossman, Harry Herr, Pierre Karakiewicz, et al. Epidemiology and Risk Factors of Urothelial Bladder Cancer. European Urology. Elsevier; 2013;63(2):234–241.
2. Marcus GK Cumberbatch, Ibrahim Jubber, Peter C Black, Francesco Esperto, Jonine D Figueroa, Ashish M Kamat, et al. Epidemiology of Bladder Cancer: A Systematic Review and Contemporary Update of Risk Factors in 2018. European Urology. Elsevier; 2018;74(6):784–795.
3. Neal D Freedman, Debra T Silverman, Albert R Hollenbeck, Arthur Schatzkin, Christian C Abnet. Association between smoking and risk of bladder cancer among men and women. Jama. American Medical Association; 2011;306(7):737–745.
4. NCI. SEER Cancer Stat Facts: Bladder Cancer 2019 [Internet]. 2019. Available from: https://seer.cancer.gov/statfacts/html/urinb.html

5. Rebecca L Siegel, Kimberly D Miller, Hannah E Fuchs, Ahmedin Jemal. Cancer Statistics, 2022. CA: A Cancer Journal for Clinicians. 2022;72(1).
6. Virginia A Moyer. Screening for bladder cancer: US Preventive Services Task Force recommendation statement. Annals of internal medicine. American College of Physicians; 2011;155(4):246–251.

Brown University
Model Overview

Model Overview

Summary

This section provides an overview of the Kystis model structure and its components.

Purpose

Kystis describes the natural history of bladder cancer and the impact of existing or emerging technologies for its prevention, control, and management. See Model Purpose for more details.

Background

Bladder cancer is the sixth most common cancer in the U.S. and the fourth leading cause of cancer deaths in men, with over 83,700 new cases and 17,200 deaths annually.[1,2] The incidence of bladder cancer peaks after age 70 and is about three times higher in men than in women.[2-5] It is more commonly diagnosed in Non-Hispanic White persons compared to Non-Hispanic Black, Asian, or Hispanic persons.[2] However Non-Hispanic Black and Hispanic people are more likely to be diagnosed at a later stage and have worse outcomes.[6-8] On a per-patient basis, bladder cancer is the most expensive cancer to manage, surpassing colorectal, breast, prostate, and lung cancers.[9,10] Risk factors include environmental exposures such as cigarette smoking and chemical carcinogens found in the workplace or ingested, as well as genetic abnormalities.[11] Unlike other common cancers, the incidence and mortality rates of BC have remained relatively stable over the past fifty years.[1] The development of novel biomarkers and new treatments, including immunotherapies (checkpoint inhibitors), gene therapies, and antibody-drug conjugates, is expected to have a significant impact on bladder cancer epidemiology in the coming years.[12-14]

Model Description

Kystis is a microsimulation model where events are simulated in continuous time. It can simulate the natural history of bladder cancer, exposures to environmental carcinogens (primarily smoking), and bladder cancer diagnosis, treatments, surveillance, and mortality in the U.S. population. The model simulates individuals with demographic attributes and bladder cancer risk factors, generate lesions and their trajectories.

Kystis models a series of events in parallel or sequentially (**Figure 1**). Hypothetical persons are instantiated with a sex and race category and a birthdate – typically the midpoint (June 30) of a calendar year. The model simulates mortality from other causes and exposure history in parallel from a person's birth. The lesion instantiation process begins when a person enters the simulation (spawn moment) and ends with a terminal event (death from bladder cancer or other causes). A person may develop zero, one, or several lesions. The risk of lesion development is a function of demographic attributes and exposure history. Once a lesion develops, it grows and progresses through a series of states, including death from bladder cancer as a terminal state. Lesion growth and transitions impact symptom development, which in turn affects the clinical detection of bladder cancer.

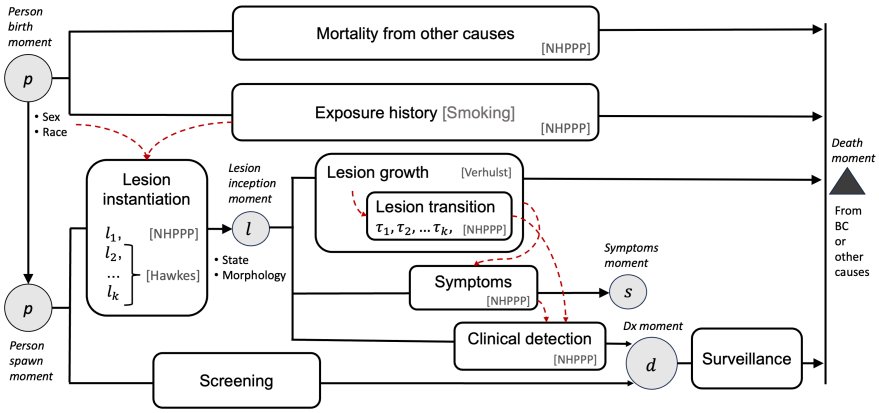

Figure 1. Modeled processes in Kystis.

Implementation

`Kystis` is implemented in `R`. Users interface with a small set of classes that encapsulate all functionality:

- The `Population` class handles the simulation of the natural history of bladder cancer and the history of environmental exposures in a group of people. It includes methods to set up groups with user-defined demographics (birthdate, sex, race), and simulates their smoking and other exposure histories; initiates bladder cancer lesions and their evolution; and tracks symptoms and clinical diagnoses in individuals with bladder cancer.
- The `LesionSet` class handles the complete counterfactual history for the evolution of each lesion from its inception, to possibly, bladder cancer death.
- The states that bladder lesions can take and the allowed transitions between the lesion states are prescribed by the `StatesGraph` class. This object includes a graph of lesion states, with edges for the allowable transitions.
- An `RNGStreams` class instantiates independent random number streams that enables using Common Random Numbers or Antithetic Random Numbers for different parts of the simulation, using the L'Ecuyer-Lécot generator.[15,16] For example, there are different random number streams for smoking exposures, other toxin exposures, background mortality, lesion generation, lesion progression, testing strategies and treatment strategies.
- The `Simulator` class is responsible for setting up and running a simulation and, as needed, updating the simulation to run with alternative scenarios.
- The `Calibrator` class provides a convenient interface for handling calibration tasks. It generates calibration designs *de novo* or augments an existing design using various methods; updates the simulated population for (a subset of) the design, records results, and evaluates objective functions.

`Kystis` is implemented in `R` as a standalone package. The model is fully vectorized and some of its calulations are multi-threaded. A set of ancillary `R` packages abstract functionality that can be used by other models or more generally, and are imported into `Kystis`. Specifically,

- The `nhppp` package implements high performance algorithms written in `C` and `C++` for the vectorized simulation of event times from non-Homogeneous Poisson Point Processes. Simulating point processes is the computational workhorse with user-specified intensity and cumulative intensity functions.[17,18]
- The `mortality` package, which simulates death from any cause in the U.S. population based on historic data from various user-selectable sources.

- Exposure generators, currently represented by `smokingHxGen`, an extensively verified mathematically and numerically equivalent adaptation of the CISNET Lung Group Smoking History Generator version 5.2.1.[19]

Modules for bladder cancer screening, surveillance, and treatment are under development.

References

1. NCI. SEER Cancer Stat Facts: Bladder Cancer 2019 [Internet]. 2019. Available from: https://seer.cancer.gov/statfacts/html/urinb.html
2. Rebecca L Siegel, Kimberly D Miller, Hannah E Fuchs, Ahmedin Jemal. Cancer Statistics, 2022. CA: A Cancer Journal for Clinicians. 2022;72(1).
3. Maximilian Burger, James WF Catto, Guido Dalbagni, H Barton Grossman, Harry Herr, Pierre Karakiewicz, et al. Epidemiology and Risk Factors of Urothelial Bladder Cancer. European Urology. Elsevier; 2013;63(2):234–241.
4. Marcus GK Cumberbatch, Ibrahim Jubber, Peter C Black, Francesco Esperto, Jonine D Figueroa, Ashish M Kamat, et al. Epidemiology of Bladder Cancer: A Systematic Review and Contemporary Update of Risk Factors in 2018. European Urology. Elsevier; 2018;74(6):784–795.
5. Jakub Dobruch, Siamak Daneshmand, Margit Fisch, Yair Lotan, Aidan P Noon, Matthew J Resnick, et al. Gender and Bladder Cancer: A Collaborative Review of Etiology, Biology, and Outcomes. European Urology. Elsevier; 2016;69(2):300–310.
6. Adam B Weiner, Mary-Kate Keeter, Adarsh Manjunath, Joshua J Meeks. Discrepancies in staging, treatment, and delays to treatment may explain disparities in bladder cancer outcomes: an update from the National Cancer Data Base (2004–2013). Urologic Oncology: Seminars and Original Investigations. Elsevier; 2018. p. 237-e9.
7. Yu Wang, Qian Chang, Yang Li. Racial differences in urinary bladder cancer in the United States. Scientific Reports. Nature Publishing Group UK London; 2018;8(1):12521.
8. Wesley Yip, Giovanni Cacciamani, Sumeet K Bhanvadia. Disparities in bladder cancer outcomes based on key sociodemographic characteristics. Current Urology Reports. Springer; 2020;21:1–6.
9. Elenir BC Avritscher, Catherine D Cooksley, H Barton Grossman, Anita L Sabichi, Lois Hamblin, Colin P Dinney, et al. Clinical Model of Lifetime Cost of Treating Bladder Cancer and Associated Complications. Urology. Elsevier; 2006;68(3):549–553.
10. Robert S Svatek, Brent K Hollenbeck, Sten Holmäng, Richard Lee, Simon P Kim, Arnulf Stenzl, et al. The Economics of Bladder Cancer: Costs and Considerations of Caring for This Disease. European Urology. Elsevier; 2014;66(2):253–262.
11. Marcus GK Cumberbatch, Aidan P Noon. Epidemiology, Aetiology and Screening of Bladder Cancer. Translational Andrology and Urology. AME Publications; 2019;8(1):5.
12. Dharmesh Gopalakrishnan, Vadim S Koshkin, Moshe C Ornstein, Athanasios Papatsoris, Petros Grivas. Immune Checkpoint Inhibitors in Urothelial Cancer: Recent Updates and Future Outlook. Therapeutics and Clinical Risk Management. Taylor & Francis; 2018;14:1019–1040.
13. Jonathan J Duplisea, Sharada Mokkapati, Devin Plote, Kimberly S Schluns, David J McConkey, Seppo Yla-Herttuala, et al. The development of interferon-based gene therapy for BCG unresponsive bladder cancer: from bench to bedside. World Journal of Urology. Springer; 2019;37:2041–2049.
14. Panagiotis J Vlachostergios, Christopher D Jakubowski, Muhammad J Niaz, Aileen Lee, Charlene Thomas, Amy L Hackett, et al. Antibody-drug conjugates in bladder cancer. Bladder Cancer. IOS Press; 2018;4(3):247–259.
15. Jack PC Kleijnen. Antithetic variates, common random numbers and optimal computer time allocation in simulation. Management Science. INFORMS; 1975;21(10):1176–1185.
16. Pierre L'Ecuyer, Christian Lécot, Bruno Tuffin. A randomized quasi-Monte Carlo simulation method for Markov chains. Operations research. INFORMS; 2008;56(4):958–975.
17. Thomas A Trikalinos, Yuliia Sereda. The nhppp package for simulating non-homogeneous Poisson point processes in R. PLoS One. Public Library of Science San Francisco, CA USA; 2024;19(11):e0311311.
18. Thomas A Trikalinos, Yuliia Sereda. nhppp: Simulating Nonhomogeneous Poisson Point Processes in R. arXiv preprint arXiv:240200358. 2024;

19. Jihyoun Jeon, Rafael Meza, Martin Krapcho, Lauren D Clarke, Jeff Byrne, David T Levy. Chapter 5: Actual and counterfactual smoking prevalence rates in the US population via microsimulation. Risk Analysis: An International Journal. Wiley Online Library; 2012;32:S51–S68.

Brown University
Assumption Overview

BROWN

Assumption Overview

Summary

This section is an overview of assumptions for the `Kystis` natural history model.

Background

`Kystis` simulates persons who have a urinary bladder. As persons age, and depending on their exposure histories and baseline risk, lesions may appear on the surface of the bladder. Lesions grow following one of four growth patterns that correspond to the WHO 2004 classification of urothelial and non-urothelial carcinomas. Lesions with different growth patterns have different growth curves, morphology, and invasive potential. Symptoms may appear depending on the lesions' size, location (e.g., involving the trigone of the bladder), and morphology.

Assumption Listing

Sampling times

We use Nonhomogeneous Poisson Point Processes (NHPPP) to sample event times. An NHPPP has the properties that the number of events in all non-overlapping time intervals are independent random variables and that, within each time interval, the number of events is Poisson distributed. `Kystis` model utilizes *nhppp* package to generate event times using the following algorithms: (i) time-transformation of a homogeneous Poisson process via the inverse of the integrated intensity function, and (ii) thinning of a majorizing NHPPP via an acceptance-rejection scheme.[1,2]

Lesion risk

We model the occurrence of lesions using NHPPPs. Let t measure time for the n-th person. We assume that the numbers of lesions in any finite set of non-overlapping time intervals are independent random variables, and that the number of lesions at any interval has a Poisson distribution. The instantaneous rate function of the process is a continuous positive function that is bounded on any finite interval.

$$\lambda_n(t) = \exp\left(\text{BASELINE}_n + \alpha_{\text{sex}}\text{sex}_n + \alpha_{\text{race}}\text{race}_n + \sum_{g\in\mathcal{G}_a}\alpha_{\text{age},g}\mathbb{1}(\text{age}_n(t)\in\text{age\_group}_g) + \text{SMOKING}_n(t) + \text{TOXINS}_n(t)\right)$$

Above, $\mathbb{1}(\cdot)$ is the indicator function, $\mathcal{G}_a$ is the set of covariates encoding age. The risk contribution $BASELINE_n(t)$ may include genetic information and it is currently limited to having Lynch Syndrome vs not. $SMOKING_n(t)$ encodes smoking status or intensity variables. $TOXINS_n(t)$ encodes environmental exposure histories, which are under development. These risk contributions have the following functional forms:

$BASELINE_n = \alpha_{0n} + \alpha_{Lynch}\ Lynch_n\alpha_{0n} \sim N(\mu_{\alpha,baseline}, \sigma^2_{\alpha,baseline})$
$SMOKING_n(t) = \sum_{g\in\mathcal{G}_s}\alpha_{smoking,g}\ smoking_{n,g}(t)$
$TOXINS_n(t) = \sum_{g\in\mathcal{G}_x}\alpha_{toxins,g}\ toxins_{n,g}(t)$

where, $\mu_{\alpha,baseline}, \sigma^2_{\alpha,baseline}$ are hyperparameters for the random intercept, and $\mathcal{G}_s$ and $\mathcal{G}_x$ are sets of covariates encoding smoking and environmental exposures, respectively.

The integrated rate of the process in the interval $(t_0, t]$ is the bounded non-decreasing function $\Lambda_n(t_0, t) = \int_{t_0}^{t}\lambda_n(s)\ d(s)$.

It is the expected number of lesions in $(t_0, t]$.

Lesion growth

We use a Verhulst model to simulate lesion growth.[3] We assume that the rate of tumor growth (in terms of number of cells per year) is
$N(t) = \frac{N_0 e^{rt}}{1+N_0(e^{rt}-1)/N_\infty}$,

where $N_0 = N(0)$ is the tumor's cell population at time 0, r is a proportionality constant with units $year^{-1}$, and N_∞ is the "carrying capacity" of the tumor, or the maximum number of cells that the tumor can attain (measured in cells). If the starting size N_0 and the maximum size N_∞ of the lesion are fixed, the growth curve depends only on the parameter r.

The time t_z, measured in $days$, needed to reach a critical number of cells N_z is obtained from
$t_z = r^{-1}\left(\log\frac{N_\infty - N_0}{N_0} - \log\frac{N_\infty - N_z}{N_z}\right)$.

In the beginning the growth is almost exponential. The growth curve is convex until the inflection point at $N_\infty/2$ and then it becomes concave approaching asymptotically the carrying capacity N_∞.

We make the following assumptions for the growth curve:

1. We instantiate lesions a size of 10^6 cells, which corresponds to a volume of $1\ mm^3$.[4]
2. The carrying capacity for VLIP, HIP, NUC is assumed to be about $1.8 \cdot 10^{11}$ cells, corresponding to a spherical tumor of radius $3.5\ cm$.
3. The carrying capacity for CIS is assumed to be $4.57 \cdot 10^8$ cells. This corresponds to a CIS covering half of the bladder surface at a depth of 3 cellular layers.[5]
4. VLIP, HIP, and NUC lesions become visible when they are about $3\ mm$ in diameter, which corresponds to a size of $1.18 \cdot 10^8$ cells.
5. CIS lesions are assumed to become visible when they occupy an area of $0.45\ cm^2$ (roughly 7-8 mm circumscribed circle diameter), which is the average size of a tile. This corresponds to approximately $1.35 \cdot 10^6$ cells - so CIS becomes visible soon after it appears.
6. Lesions become visible after $4.60616/r_c$ years for $c \in \{\text{VLIP}, \text{HIP}, \text{NUC}\}$ and after $0.30014/r_{\text{CIS}}$ years for CIS.
7. **An average growth rate for bladder cancer lesions has been estimated at $r_c \approx 0.043\ day^{-1}$ for all c.[6] This would suggest that from inception, non-CIS lesions would become visible within approximately 107 days (3.6 months), but CIS lesions would be visible at inception (more accurately, after about 7 days).**

Lesion starting states and transitions

Figure 1 shows the modeled transitions from lesion inception to death from bladder cancer. Lesions first appear in states 0, 1, 2, 4, 6, or 8. Arrows represent allowable transitions that follow a NHPPP law. PUMLNPs (state 0) do not commonly advance to Ta lesions.[5] VLIP lesions (state 1) do not transition to other states. However they can grow in size and give symptoms like all other lesions.

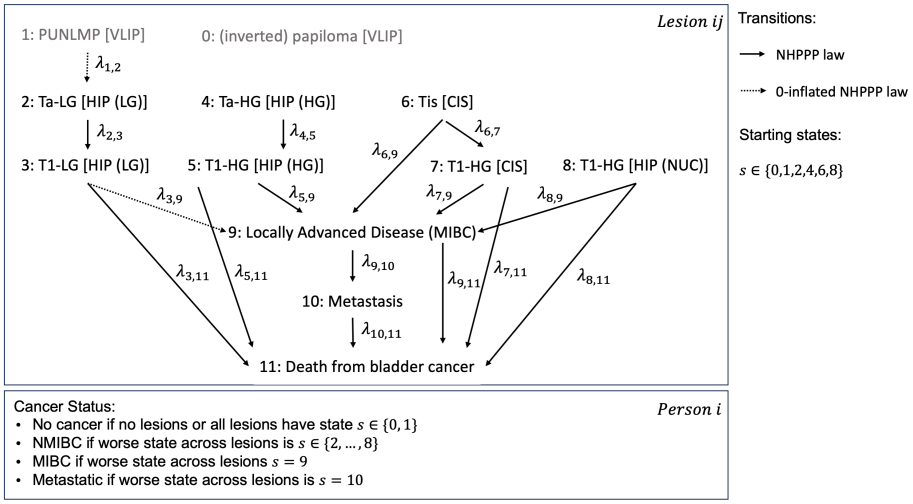

Figure 1. Transitions between states for lesions in *Kystis* and designation of cancer status at the person level.

We assume that

- HIP (HG) is more aggressive than HIP (LG) of the same size, so that $\zeta_{4,5} > \zeta_{2,3}$ and $\zeta_{5,9} \geq \zeta_{3,9}$.
- We assume that NUC is at least as aggressive as HIP (HG) of the same size, so that $\zeta_{8,9} \geq \zeta_{4,5}$ and $\zeta_{8,9} \geq \zeta_{5,9}$
- CIS lesions are flat and their tumor cell size tends to be smaller that that of other growth patterns. For example, for CIS the carrying capacity is $N_\infty \approx 4.57 \cdot 10^8$ cells, where as for other growth patterns $N_\infty \approx 1.8 \cdot 10^{11}$ cells. Thus the ζ's for CIS are not explicitly constrained with respect to those of the other growth patterns and are set through calibration.

The instantaneous rates for transitions are a function of the size of the lesion.
$\lambda_{ij}(t) = \zeta_{ij} \log(N(t)),\ \text{with } \zeta_{ij} > 0$

Transitions from PUMLNP to Ta-LG ($1 \to 2$) are considered uncommon.[5] Analogously, transitions from low grade tumors to Advanced disease may be uncommon or rare. Such uncommon or rare transitions are modelled with zero-inflated NHPPP.
$z \sim Bernoulli(\Pr[i \to j])$,
$\lambda_{ij}(t) = z\, \zeta_{ij}\ \log\left(N(t)\right), \text{with } \zeta_{ij} > 0\,,$

where the probability that a transition will occur $\Pr[i \to j]$ is obtained via calibration.

Symptom onset

We make the following assumptions:

- The majority of patients who present with symptoms have gross hematuria (80%); we assume that the rest report primarily symptoms during micturition.[5]
- A person becomes symptomatic when they develop either hematuria or symptoms during micturition.
- The probability of hematuria is related to the size of individual lesions.
- The probability of symptoms during micturition is related to
    1. the fraction of the total surface area of the bladder that is occupied by at least one lesion.
    2. the fraction of the surface area of the trigone that is occupied by at least one lesion
- We assume that we can model onset of symptoms and clinical detection using NHPPP.

Onset of voiding symptoms

The time that the n-th person will experience voiding symptoms is measured on a person clock starting from the instantiation of the first lesion ($t > t_{l1}$).

We assume that the time to symptom onset is modeled with a NHPPP with instantaneous rate $\eta_m(t) = \exp(\delta_{m0} + \delta_{m1}\, S_{bladder}^{-1} \sum_{j \in \mathcal{J}_t} S_j(t) + \delta_{m2}\, S_{trigone}^{-1} \sum_{j \in \mathcal{J}_t} S_{trig,j}(t))$.

Above, j indexes lesions in $\mathcal{J}_t$, $\mathcal{J}_t$ is the set of lesions that are present at time t, and involve at least $S_{min} = 1\ cm^2$ on the surface of the bladder, $S_j(t)$ is the area of the bladder's surface that is occupied by lesion j, and $S_{trig,j}(t)$ is the area of the trigone that is occupied by lesion j. The coefficients $\delta_{m1} > 0$ and $\delta_{m2} > 0$ determine the association between symptoms during micturition and the proportion of the surface of the bladder of the trigone that is occupied by a lesion, and δ_{m0} is an intercept term.
To facilitate calibration, we assume that $\delta_1 = \delta_2$ are global constants.

Onset of macroscopic hematuria

For the j-thlesion of the n-th person we model the onset of macroscopic hematuria, as measured on the lesion clock, as the first event from a NHPPP with instantaneous rate
$\eta_h(t) = \exp(\delta_{h0} + \delta_h \cdot \log\left(N_j(t)\right))$,

where the coefficient $\delta_h > 0$ determines the association between symptoms of hematuria and the size of the lesion. To facilitate calibration, we assume that the intercept δ_{h0} and δ_h are fixed parameters.

Clinical detection

The probability of clinical detection by time t, measured on the person clock starting from the instantiation of the first lesion t_{l1}. It is modelled as the time to the first event in a NHPPP with instantaneous rate
$\eta_s(t) = \exp\left(\delta_{s1} + \delta_{s2}\mathbb{1}(sex = \text{Female}) + \delta_{s3}\mathbb{1}(race = \text{Black}) + \delta_{s4}(t - t_{\text{micturition}})_+ + \delta_{s5}(t - t_{\text{hematuria}})_+\right)$
,

where t is measured on the person clock, $(t - t_{\text{micturition}})_+$, is the time after the onset of voiding symptoms and zero otherwise, and $(t - t_{\text{hematuria}})_+$ the time after the earliest onset of hematuria symptoms and 0 otherwise. We assume that delays in diagnosis are in part a misattribution of symptoms to urinary infections (for women) or barriers to seeking care (in Black individuals).[7]

Sojourn time

The sojourn time is the length of the time interval between the moment that a malignant lesion j becomes detectable by cystoscopy, $t_{cystoscopy\_detectable,j}$, and the time that a person is symptomatic and has clinically detectable cancer, $t_{clinical\_detection}$. It is defined for lesions that have muscle-invasive potential. It is not modeled explicitly, but it is calculated based on other quantities.

Time to death

We assume that a person can die from causes related to bladder cancer and other causes. We model time to each cause of death with competing NHPPP. The earliest time of death (due to bladder cancer or other causes) is the one that is realized. Another assumption is that death from other causes than bladder cancer is approximately equal to that of all causes in the general population stratified by age, sex, race, and smoking history.

When modeling time to death from bladder cancer, we assume that: (i) patients with NMIBC or earlier stages of the disease have a very low probability of dying from bladder cancer; (ii) patients die of bladder cancer if they have MIBC or metastatic disease; and (iii) patients with metastatic disease experience shorter bladder cancer survival rates.

References

1. Thomas A Trikalinos, Yuliia Sereda. The nhppp package for simulating non-homogeneous Poisson point processes in R. PLoS One. Public Library of Science San Francisco, CA USA; 2024;19(11):e0311311.

2. Thomas A Trikalinos, Yuliia Sereda. nhppp: Simulating Nonhomogeneous Poisson Point Processes in R. arXiv preprint arXiv:240200358. 2024;
3. Nicolas Bacaër. Verhulst and the logistic equation (1838). A short history of mathematical population dynamics. London: Springer London; 2011. p. 35–39.
4. John A Spratt, D Von Fournier, John S Spratt, Ernst E Weber. Decelerating growth and human breast cancer. Cancer. Wiley Online Library; 1993;71(6):2013–2019.
5. Petrisor Aurelian Geavlete. Endoscopic Diagnosis and Treatment in Urinary Bladder Pathology: Handbook of Endourology. Academic Press; 2016.
6. Cyrill A Rentsch, Claire Biot, Joël R Gsponer, Alexander Bachmann, Matthew L Albert, Romulus Breban. BCG-Mediated Bladder Cancer Immunotherapy: Identifying Determinants of Treatment Response Using a Calibrated Mathematical Model. PloS one. 2013 Feb;8(2):e56327-17.
7. NCI. SEER Cancer Stat Facts: Bladder Cancer 2019 [Internet]. 2019. Available from: https://seer.cancer.gov/statfacts/html/urinb.html

Parameter Overview

Summary

Describes the basic parameter set used to inform the model, more detailed information is available for each specific parameter.

Background

The `Kystis` model uses two types of parameters:

- **Fixed parameters**: These include global constants such as the maximum age of a person or baseline specifications of the urinary bladder. These parameters are detailed in the Component Overview.
- **Calibrated parameters** These parameters are used to define and adjust model processes, such as how lesions start and progress. They are fine-tuned to ensure the model's output closely matches observed data. This page focuses on calibrated parameters.

For more information on the equations used, refer to the Assumption Overview.

Parameter Listing Overview

Table 1 summarizes the parameters used in the Kystis model to simulate bladder cancer onset, lesion growth and transitions, symptom development, and clinical detection.

- *Lesion instantiation* rate depends on factors such as sex, race, age, and exposure history. Exposure history is limited to smoking in the current version of the model and accounts for both smoking status and smoking intensity. The age is modeled as a continuous covariate with additional risk after specific age thresholds (i.e., greater than {50,55,60,65,70,75,80,85}). The risk is capped at older ages (`truncation_age`) to match the plateau observed in age-specific bladder cancer incidence curves. Lesion instantiation parameters vary by the tumor grade (low or high grade).
- *Lesion growth* is a Verhulst model, which is based on a time-varying tumor growth rate measured in the number of cells per day. Two additional parameters (`growth_mult_VLIP` and `growth_mult_HIP_LG`) scale growth curves for lesions with VLIP and HIP growth patterns.
- *Voiding symptoms* rate is a function of lesion spread on the urinary bladder surface. Lesions located at the bladder trigone are assumed to increase the likelihood of voiding symptoms.
- *Macroscopic bleeding* is modeled as a function of lesion size measured in cells.
- *Bladder cancer clinical detection* depends on the time since symptom onset (if symptoms are present), sex, race, and the development of advanced disease (e.g., MIBS or metastasis).
- *Lesion transitions* are modeled using a graph consisting of vertices (nodes) and edges connecting pairs of vertices. Vertex parameters include the names of allowed states, starting state probabilities, and morphology probabilities. There are 16 allowed edges in the graph, each as a function of lesion size. Two edges ('PUNLMP [VLIP]' to 'Ta-LG [HIP LG]' and 'T1-LG [HIP LG]' to 'Locally advanced disease') are considered uncommon and are modeled with zero-inflated NHPPP, using zero mass probability as an additional parameter.

Table 1. `Kystis` calibrated parameters.

A. Lesion instantiation.

Parameter	Hyperparameters	Description
`intercept`	$N(\mu, \sigma^2)$	Log risk of bladder cancer among unexposed White Men at birth
`lynch_syndrom`	$N(\mu, \sigma^2)$	Change in log risk of bladder cancer for Lynch syndrome vs. not
`sex_female`	$N(\mu, \sigma^2)$	Change in log risk of bladder cancer for Female vs. Male biological sex
`race_black`	$N(\mu, \sigma^2)$	Change in log risk of bladder cancer for Black vs. White Race

Parameter	Hyperparameters	Description
age	$U(a,b)$	Change in log risk of bladder cancer per unit [year] increase in age, for ages below truncation_age
age_ge_X	$N(\mu,\sigma^2)$	If age is ≥ X years, these terms add a constant value to the log risk of bladder cancer
truncation_age	$U(a,b)$	Age beyond which bladder cancer risk is capped
past_smoker	$N(\mu,\sigma^2)$	Change in log risk of bladder cancer for former smokers vs. not
smoking_exposure	$N(\mu,\sigma^2)$	Change in log risk of bladder cancer per unit increase in smoking cumulative intensity
toxin_exposure	$N(\mu,\sigma^2)$	Change in log risk of bladder cancer per unit increase in toxin cumulative intensity

B. Lesion growth.

Parameter	Hyperparameters	Description
growth_rate	$U(a,b)$	Rate of tumor growth, number of cells per day
growth_mult_VLIP	$U(a,b)$	Multiplyer for the rate of tumor growth in lesions with VLIP growth pattern
growth_mult_HIP_LG	$U(a,b)$	Multiplyer for the rate of tumor growth in low-grade lesions with HIP growth pattern
log_N0	$U(a,b)$	Log of tumor's cell population at time 0
N0_to_Ninf_ratio_nonCIS	$U(a,b)$	Ratio of tumor's cell population at time 0 and the maximum number of cells that the tumor can attain (measured in cells) in lesions with VLIP, HIP or NUC growth pattern
N0_to_Ninf_ratio_CIS	$U(a,b)$	Ratio of tumor's cell population at time 0 and the maximum number of cells that the tumor can attain (measured in cells) in lesions with CIS growth pattern

C. Voiding symptoms.

Parameter	Hyperparameters	Description
intercept	$U(a,b)$	Risk of voiding symptoms at lesion instantiation
S_bladder_fraction	$U(a,b)$	Risk of voiding symptoms per unit change in the area of the bladder's surface that is occupied by lesion
S_trigone_fraction	$U(a,b)$	Risk of voiding symptoms per unit change in the area of the bladder's trigone that is occupied by lesion

D. Macroscopic bleeding.

Parameter	Hyperparameters	Description
intercept	$U(a,b)$	Risk of macroscopic bleeding at lesion instantiation
logN	$U(a,b)$	Risk of macroscopic bleeding per unit change in the log of tumor's cell population

E. Clinical detection.

Parameter	Hyperparameters	Description
intercept	$U(a,b)$	Risk of clinical detection of NMIBC in White Males without symptoms
sex_female	$U(a,b)$	Change in risk of clinical detection for Female vs. Male biological sex
race_black	$U(a,b)$	Change in risk of clinical detection for Black vs. White Race
macroscopic_bleeding	$N(\mu,\sigma^2)$	Change in risk of clinical detection per unit increase in time since macroscopic bleeding started or zero otherwise
voiding_symptoms	$N(\mu,\sigma^2)$	Change in risk of clinical detection per unit increase in time since voiding symptoms started or zero otherwise
mibc	$U(a,b)$	Change in risk of clinical detection for developing MIBC vs. NMIBC or precancerous states
metastasis	$U(a,b)$	Change in risk of clinical detection for developing metastatic disease vs. NMIBC or precancerous states

F. Lesion graph vertices.

Parameter	Hyperparameters	Description
prop_LG	$U(a, b)$	Proportion of low grade lesions at lesion instantiation
state_names	{'Papilloma [VLIP]', 'PUNLMP [VLIP]', 'Ta-LG [HIP LG]', 'T1-LG [HIP LG]', 'Ta-HG [HIP HG]', 'T1-HG [HIP HG]', 'Tis [CIS]', 'T1-HG [CIS]', 'T1-HG [NUC]', 'Locally advanced disease', 'Metastasis', 'BC death'}	Allowed lesion states
starting_state_probs	{0, 0, 0.675, 0, 0.225, 0, 0.09, 0, 0.01, 0, 0, 0}	Probabilities of lesion states at onset, in the order of state_names
flat_morphology_probs	{0, 0, 0, 0, 0, 0, 1, 0, 0, 0, 0, 0}	Probabilities of flat morphology at lesion onset, in the order of state_names
stalked_morphology_probs	{1, 1, 0.8, 0.8, 0.2, 0.2, 0, 0.2, 0, 0, 0, 0}	Probabilities of stalked morphology at lesion onset, in the order of state_names

G. Lesion graph edges.

Parameter	Hyperparameters	Description
punlmp__to__talg_logN	$U(a, b)$	Change in risk of lesion transition from 'PUNLMP [VLIP]' to 'Ta-LG [HIP LG]' per unit increase in log of lesion size measured in cells
talg__to__t1lg_logN	$U(a, b)$	Change in risk of lesion transition from 'Ta-LG [HIP LG]' to 'T1-LG [HIP LG]' per unit increase in log of lesion size measured in cells
t1lg__to__lad_logN	$U(a, b)$	Change in risk of lesion transition from 'T1-LG [HIP LG]' to 'Locally advanced disease' per unit increase in log of lesion size measured in cells
t1lg__to__bcdeath_logN	$U(a, b)$	Change in risk of lesion transition from 'T1-LG [HIP LG]' to 'BC death' per unit increase in log of lesion size measured in cells
tahg__to__t1hg_logN	$U(a, b)$	Change in risk of lesion transition from 'Ta-HG [HIP HG]' to 'T1-HG [HIP HG]' per unit increase in log of lesion size measured in cells
t1hg__to__lad_logN	$U(a, b)$	Change in risk of lesion transition from 'T1-HG [HIP HG]' to 'Locally advanced disease' per unit increase in log of lesion size measured in cells
t1hg__to__bcdeath_logN	$U(a, b)$	Change in risk of lesion transition from 'T1-HG [HIP HG]' to 'BC death' per unit increase in log of lesion size measured in cells
tis__to__t1cis_logN	$U(a, b)$	Change in risk of lesion transition from 'Tis [CIS]' to 'T1-HG [CIS]' per unit increase in log of lesion size measured in cells
tis__to__lad_logN	$U(a, b)$	Change in risk of lesion transition from 'Tis [CIS]' to 'Locally advanced disease' per unit increase in log of lesion size measured in cells
t1cis__to__lad_logN	$U(a, b)$	Change in risk of lesion transition from 'T1-HG [CIS]' to 'Locally advanced disease' per unit increase in log of lesion size measured in cells
t1cis__to__bcdeath_logN	$U(a, b)$	Change in risk of lesion transition from 'T1-HG [CIS]' to 'BC death' per unit increase in log of lesion size measured in cells
t1nuc__to__lad_logN	$U(a, b)$	Change in risk of lesion transition from 'T1-HG [NUC]' to 'Locally advanced disease' per unit increase in log of lesion size measured in cells
t1nuc__to__bcdeath_logN	$U(a, b)$	Change in risk of lesion transition from 'T1-HG [NUC]' to 'BC death' per unit increase in log of lesion size measured in cells
lad__to__meta_logN	$U(a, b)$	Change in risk of lesion transition from 'Locally advanced disease' to 'Metastasis' per unit increase in log of lesion size measured in cells
lad__to__bcdeath_logN	$U(a, b)$	Change in risk of lesion transition from 'Locally advanced disease' to 'BC death' per unit increase in log of lesion size measured in cells
meta__to__bcdeath_logN	$U(a, b)$	Change in risk of lesion transition from 'Metastasis' to 'BC death' per unit increase in log of lesion size measured in cells
punlmp__to__talg_pr0mass	$U(a, b)$	Probability of observing no transitions from 'PUNLMP [VLIP]' to 'Ta-LG [HIP LG]' in a given interval in zero-inflated NHPPP
talg__to__t1lg_pr0mass	$U(a, b)$	Probability of observing no transitions from 'Ta-LG [HIP LG]' to 'T1-LG [HIP LG]' in a given interval in zero-inflated NHPPP
t1lg__to__lad_pr0mass	$U(a, b)$	Probability of observing no transitions from 'T1-LG [HIP LG]' to 'Locally advanced disease' in a given interval in zero-inflated NHPPP

Parameter	Hyperparameters	Description
t1lg__to__bcdeath_pr0mass	$U(a, b)$	Probability of observing no transitions from 'T1-LG [HIP LG]' to 'BC death' in a given interval in zero-inflated NHPPP
tahg__to__t1hg_pr0mass	$U(a, b)$	Probability of observing no transitions from 'Ta-HG [HIP HG]' to 'T1-HG [HIP HG]' in a given interval in zero-inflated NHPPP
t1hg__to__lad_pr0mass	$U(a, b)$	Probability of observing no transitions from 'T1-HG [HIP HG]' to 'Locally advanced disease' in a given interval in zero-inflated NHPPP
t1hg__to__bcdeath_pr0mass	$U(a, b)$	Probability of observing no transitions from 'T1-HG [HIP HG]' to 'BC death' in a given interval in zero-inflated NHPPP
tis__to__t1cis_pr0mass	$U(a, b)$	Probability of observing no transitions from 'Tis [CIS]' to 'T1-HG [CIS]' in a given interval in zero-inflated NHPPP
tis__to__lad_pr0mass	$U(a, b)$	Probability of observing no transitions from 'Tis [CIS]' to 'Locally advanced disease' in a given interval in zero-inflated NHPPP
t1cis__to__lad_pr0mass	$U(a, b)$	Probability of observing no transitions from 'T1-HG [CIS]' to 'Locally advanced disease' in a given interval in zero-inflated NHPPP
t1cis__to__bcdeath_pr0mass	$U(a, b)$	Probability of observing no transitions from 'T1-HG [CIS]' to 'BC death' in a given interval in zero-inflated NHPPP
t1nuc__to__lad_pr0mass	$U(a, b)$	Probability of observing no transitions from 'T1-HG [NUC]' to 'Locally advanced disease' in a given interval in zero-inflated NHPPP
t1nuc__to__bcdeath_pr0mass	$U(a, b)$	Probability of observing no transitions from 'T1-HG [NUC]' to 'BC death' in a given interval in zero-inflated NHPPP
lad__to__meta_pr0mass	$U(a, b)$	Probability of observing no transitions from 'Locally advanced disease' to 'Metastasis' in a given interval in zero-inflated NHPPP
lad__to__bcdeath_pr0mass	$U(a, b)$	Probability of observing no transitions from 'Locally advanced disease' to 'BC death' in a given interval in zero-inflated NHPPP
meta__to__bcdeath_pr0mass	$U(a, b)$	Probability of observing no transitions from 'Metastasis' to 'BC death' in a given interval in zero-inflated NHPPP

Component Overview

Summary

A description of the basic computational building blocks (components) of the model.

Overview

`Kystis` models the natural history of bladder cancer through a combination of parallel and sequential processes. It generates a population where each person has specific demographic attributes. From birth, the model simulates mortality from causes other than bladder cancer and tracks exposure history. Individuals can develop zero, one, or multiple lesions. The process of lesion formation begins when a person enters the simulation (spawn moment) and is influenced by their demographic attributes and exposure history. Once a lesion instantiated, it grows and progresses through several stages and can ultimately result in death from bladder cancer. Lesion growth and transitions impact symptom development, which in turn affects the clinical detection of bladder cancer.

Component Listing

Time clocks

We use time clock objects to count time unambiguously. These objects have an internal representation that is concordant with ISO 8601.[1] They have a common origin date, are aware of time units, and can be aligned with each other.

In the simulation, we measure time on *calendar*, *person* and *lesion* clocks, where for the n-th person and j-th lesion:
$\texttt{calendar\_clock(n)}.years() = \texttt{person\_clock(n)}.years() + birth\_cohort_n + sim\_start\_age_n$
$= \texttt{lesion\_clock(n, j)}.years() + birth\_cohort_n + lesion\_start\_age_{nj}$
$\texttt{person\_clock(n)}.years() = \texttt{calendar\_clock(n)}.years() - birth\_cohort_n - sim\_start\_age_n$
$= \texttt{lesion\_clock(n, j)}.years() + lesion\_start\_age_{nj} - sim\_start\_age_n$, and
$\texttt{lesion\_clock(n, j)}.years() = \texttt{calendar\_clock()}.years() - birth\_cohort_n - lesion\_start\_age_{nj}$
$= \texttt{person\_clock(n)}.years() - lesion\_start\_age_{nj} + sim\_start\_age_n$

Person

When instantiated, each simulated person has or is associated with

- a $birth\_cohort = 1920, \ldots, 2000$;
- a simulation start age, $sim\_start\_age = 40$, measured in $years$;
- a `person_clock` that measures time in the simulation;
- a biological sex, $sex \in \{\text{male, female}\}$;
- a `smoking_exposure` object that defines a smoking exposure personal history;
- a `toxin_exposure` object that defines a personal history of environmental or occupational toxin exposure;
- a `baseline_risk` object, which may include genetic information. Currently, this is limited to having Lynch Syndrome.

Urinary Bladder

Table 1 describes the parameters we chose for the simulation of a urinary bladder.

Table 1. Urinary bladder specifications.

Item or variable	Description	Value	Units	Explanation
$R_{bladder}$	Bladder sphere radius	$4.92 \cdot 10^{-2}$	m	A distended bladder is a sphere that has 500 mL capacity.
$V_{bladder}$	Bladder sphere volume	$5 \cdot 10^{-4}$	m^3	
$S_{bladder}$	Bladder sphere area	$3.05 \cdot 10^{-2}$	m^2	
M	Number of tiles	678	[tiles]	
$V(G_{678})$	Dual graph of tiling, number of vertices	678	[vertices]	As many as the tiles
$E(G_{678})$	Dual graph of tiling, number of edges	2028	[edges]	As many as the boundaries between tiles
Tiles	Area	$4.49 \cdot 10^{-5}$	m^2	
	Circumscribed circle diameter	$8.32 \cdot 10^{-3}$	m	
Trigone	Convex hull on the tesselation (vertices in G_{678})	1, 36, 86		1: urethra, 36: left ureter, 86: right ureter
	Arc length between ureteral orifices	$5.00 \cdot 10^{-2}$	m	distended
	Actual trigone arc lengths	$(5.03, 5.06, 5.16) \cdot 10^{-2}$	m	based on the tesselation
	Actual dihedral (included) angles of trigone vertices	(1.21, 1.22, 1.25)	[radians]	about 69-71 degrees
$S_{trigone}$	Area of trigone	$1.29 \cdot 10^{-3}$	m^2	$\approx 4\%$ of $S_{bladder}$

An empty bladder is approximately tetrahedral and its lining (urothelium) forms mucosal folds. As it fills, it first becomes ellipsoidal and then approximately spherical, and its folds get flattened out. We assume that a fully distended bladder (e.g., during cystoscopy) can be satisfactorily approximated with a *convex polyhedron* inscribed in a 500 mL sphere. The surface of the polyhedron approximates the surface of the bladder sphere by inducing a *polygonal tiling (tesselation)* $\mathcal{T}_M = \{\mathbf{T}_m \mid m = 1, \ldots, M\}$ of the sphere's surface, where $\mathbf{T}_m$ is the m-th facet (*tile*) and M is the total number of the facets (*tiles*) of the polyhedron.

**Figure 1 ** shows the chosen tiling $\mathcal{T}_{678}$, which has $M = 678$ tiles with mean area about 0.45 cm^2. The diameter of the circle that circumscribes each hexagonal tile is approximately 0.8 cm. The *dual graph* G_{678} of the tiling $\mathcal{T}_{678}$ has 678 vertices and 2028 edges. *Vertices* represent the centroids of the tiles and are shown as circularly-arranged small black and red dots. The three vertices that define the *trigone* (vertices 1, 36, and 86) are depicted larger and in red. *Undirected edges* (thin gray lines) connect vertices when the respective tiles share a border. Most tiles are hexagonal and have six adjacent tiles, thus most vertices have degree six.

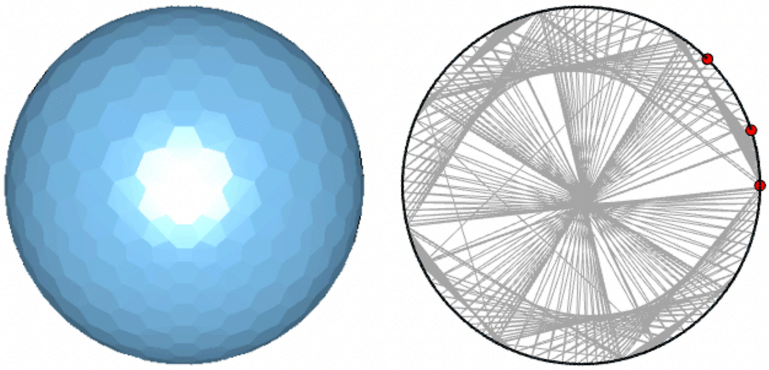

(a) $\mathcal{T}_{678}$: Tiling/polyhedral approximation of a sphere (b) G_{678}: The dual graph of the tiling $\mathcal{T}_{678}$

Figure 1. Polyhedral approximation of the urinary bladder in the *Kystis*.

Bladder cancer lesion

A person may develop zero, one or several lesions. Precursor dysplastic lesions may appear and regress or grow to become benign or malignant tumors. We do not explicitly model the process of developing and

regressing dysplastic lesions. We model lesions conditional on that they will not regress. Such a non-regressing lesion

1. Starts on a single tile.
2. Starts as a noninvasive tumor.
3. Follows one of four archetypical growth patterns, which correspond to the WHO 2004 histological grading of bladder cancer tumors:
    - CIS: urothelial carcinoma *in situ*, which has a flat morphology and grows on the surface of the bladder.
    - VLIP: very low invasive potential. This type includes the WHO 2004 categories of *papillomas*, *inverted papillomas*, and *primarily papillary urothelial neoplasia with low malignant potential (PUNLMP)*. For simplicity, all VLIP lesions are assumed to be pendunculated and papillary in appearance. Their risk of progression is assumed to be negligible.
    - HIP: higher invasive potential. This type includes urothelial neoplasias that can evolve to invasive cancer before developing symptoms. They can be papillary or non-papillary, but assumed to be more often sessile rather than pendunculated. They include lesions that will evolve to low grade and high grade papillary urothelial carcinomas (LGPUC, HGPUC).
    - NUC: non-urothelial malignancies comprising squamous cell carcinomas and adenocarcinomas. They have a more-aggressive growth curve than the HIP category, so they become invasive at an earlier tumor burden. They are assumed to be non-papillary and sessile.
4. Has a $histology \in \{\text{HG} = \text{high grade}, \text{LG} = \text{low grade}\}$. Low-grade tends to grow slowly. High-grade is more likely to grow into the bladder wall and spread outside the bladder. Histology is important in determining the probability that a HIP will become muscle invasive.
5. Has a $morphology$ that is determined by the growth pattern. In terms of configuration morphology, a lesion may be flat, papillary, or non-papillary; and in terms of stalk morphology a lesion may be pendunculated (with a stalk), sessile (protruding without a stalk) or flat (which also has no stalk). The stalk morphology determines the growth of the base area of a lesion as a function of the lesion's size or volume.
6. Has a $size$ measured in number of *cells*, which also determines a *volume* measured in mm^3. A lesion's size evolves over time following a Verhulst growth model.
7. Has a $base$, which is the part of the surface of the bladder that is occupied by the lesion. The lesion's base is represented as a set of contiguous tiles in $\mathcal{T}_M$, or, equivalently, a connected subgraph of G_M. We record which tiles of the base belong to the trigone because this is important for determining the probability of symptoms during micturition. As the lesion grows, so does its base; the growth curve for the base area is related to the growth curve of the lesion's number of cells, and the stalk morphology.

Table 2 summarizes lesion stages, corresponding grades, and growth patterns in the `Kystis` model. The AJCC TNM staging system, commonly used for bladder cancer, describes the tumor's growth pattern and extent (T), lymph node involvement (N), and metastasis (M). `Kystis` can generate precancerous (PUNLMP) and benign (papillomas) lesions. It models non-muscle invasive cancer with Ta and Tis stages, which can progress to T1. `Kystis` does not differentiate between AJCC stages of muscle invasive cancer (T2, T3) and distant metastasis (M1a, M1b), and it does not model lymph node involvement (N). Lesion transitions are described in Model Assumptions.

Table 2. Bladder cancer staging in the `Kystis`.

AJCC Staging System (8th edition, 2017)	Kystis Stage	Kystis Grade	Kystis Growth Pattern	Description
-	PUNLMP	-	VLIP	Papillary Urothelial Neoplasm of Low Malignant Potential; a pre-malignant tumor, very slow-growing and unlikely to spread.
-	Papilloma	-	VLIP	Urothelial papilloma, a rare benign tumor of the bladder.

AJCC Staging System (8th edition, 2017)	Kystis Stage	Kystis Grade	Kystis Growth Pattern	Description
Ta	Ta	Low, High	HIP	Non-invasive papillary carcinoma. It has grown toward the hollow center of the bladder but has not grown deeper into the connective tissue or muscle of the bladder wall.
Tis	Tis	-	CIS	Flat, non-invasive carcinoma. The cancer is growing in the inner lining layer of the bladder only.
T1	T1	Low, High	HIP, CIS, NUC	The cancer has grown into the layer of connective tissue under the lining layer of the bladder, but it has not reached the layer of muscle in the bladder wall.
T2a, T2b, T3a, T3b	Locally Advanced Disease (MIBC)	-	-	The cancer has grown through the muscle layer of the bladder (T2) or into the layer of fatty tissue surrounding the bladder (T3), but it has not spread to adjacent organs or distant parts of the body.
T4a, T4b, M1a, M1b	Metastasis	-	-	The cancer have spread into the prostate, seminal vesicles, uterus, vagina, pelvic or abdominal wall (T4) or to distant parts of the body (M1).

Lesion instantiation

In the `Kystis` model, the risk of lesion occurrence depends on person's demographic characteristics, such as sex, race and age, and exposure histories. We simulate lesions occurrence using non homogeneous Poisson point process (NHPPP). In an NHPPP, each event occurs independently of others, which doesn't accurately reflect the nature of cancer progression where existing lesions can influence the occurrence of new ones. Currently, we are extending the model functionality to implement Hawkes process for the generation of subsequent lesions. Hawkes process is self-exciting, meaning that each event increases the rate of future events temporarily.

Lesion growth and progression

Once a person develops a lesion, it begins to grow following the Verhulst model, also known as the logistic growth model. The lesion grows rapidly at first, then slows as it approaches its carrying capacity. For Tis lesions, the carrying capacity is the number of cells that line half the surface of the bladder. For all other tumors, it is the number of tumor cells that occupy one-third of the volume of a distended bladder. The "steepness" of the growth curve is determined by the growth rate, which varies by lesion archetype (growth pattern).

Allowed lesion states and transitions are defined by the graph object. Papillomas, PUNLMPs, Tis, and low- and high-grade Ta tumors are primary lesions. PUNLMPs are not malignant but may occasionally evolve into malignant lesions, thus constituting precursor lesions. Papillomas and inverted papillomas are modeled as benign-only lesions that can manifest clinically. In the `Kystis` model, a lesion's histologic grade is immutable once set at its inception (Ta-LG, Ta-HG). The model grows Ta lesions to T1 (T1-LG and T1-HG) without cross-transitions between the low- and high-grade paths. Tis lesions can become T1 lesions or lead directly to MIBC and then to metastatic disease. We use NHPPP to sample times of lesion transitions, where the instantaneous rate is a function of the size of the lesion.

Symptoms

The `Kystis` model includes two types of symptoms: macroscopic hematuria (blood in the urine) and irritative symptoms during urination. The instantaneous rate of voiding symptoms is influenced by the location of the lesions (whether in the trigone or elsewhere) and the total area of the bladder covered by one or more lesions. The rate of hematuria is determined by the size of the lesion. Both symptom types are simulated using NHPPP.

Clinical detection

We use NHPPP to simulate the clinical detection of bladder cancer. The instantaneous rate of clinical detection depends on sex, race, and the duration of bladder cancer symptoms, such as hematuria and voiding symptoms. Women and Black individuals tend to be diagnosed later on average due to the misattribution of symptoms to urinary infections for women or barriers to seeking care for non-Whites.[2]

Exposure history

Exposure generator is currently limited to smoking history and utilises the CISNET Lung Cancer Group Smoking History Generator (SHG).[3] The SHG simulates life histories of people born in the U.S. between 1864 and 2100, tracking them up to age of 99. These histories include the year of birth and the age of death from all causes and causes other than lung cancer, conditional on smoking exposure. For each simulated person, the SHG simulates age they started smoking, smoking intensity defined as cigarettes per day at yearly intervals, and the age they quit smoking. Outputs are stratified by sex and race. The SHG does not account for recurrent smoking.

We adapted the SHG for R programming language and introduced sampling from NHPPP to draw times of smoking initiation, smoking sessation and deaths.

Mortality

We sample death times using NHPPP based on data from the Human Mortality Database (overall mortality)[4] and the CISNET Lung Cancer Group Smoking History Generator[3] (mortality conditional on smoking history).

Bladder cancer death is modeled as one of the lesion transitions. A person can die from bladder cancer if one or more lesions progress to muscle-invasive disease or metastasis. The hazard of dying from bladder cancer at the non-muscle invasive stage (T1) is negligible; though it is still possible. The first occurrence of death, whether from bladder cancer or other causes, is the one that is taken into account.

Surveillance

The surveillance module has not been implemented yet.

Screening

The screening module has not been implemented yet.

References

1. International Organization for Standardization. International Standard for the Representation of Dates and Times: ISO 8601 [Internet]. 2020. Available from: https://www.iso.org/iso-8601-date-and-time-format.html
2. NCI. SEER Cancer Stat Facts: Bladder Cancer 2019 [Internet]. 2019. Available from: https://seer.cancer.gov/statfacts/html/urinb.html
3. Jihyoun Jeon, Rafael Meza, Martin Krapcho, Lauren D Clarke, Jeff Byrne, David T Levy. Chapter 5: Actual and counterfactual smoking prevalence rates in the US population via microsimulation. Risk Analysis: An International Journal. Wiley Online Library; 2012;32:S51–S68.
4. John R Wilmoth, Kirill Andreev, Dmitri Jdanov, Dana A Glei, C Boe, M Bubenheim, et al. Methods protocol for the human mortality database. University of California, Berkeley, and Max Planck Institute for Demographic Research, Rostock URL: http://mortality org [version 31/05/2007]. 2007;9:10–11.

Output Overview

Summary

Definitions and methodologies for the basic model outputs.

Overview

The `Kystis` model simulates the U.S. population born between 1920 and 2000, encompassing their environmental exposures and the natural history of bladder cancer. This model generates two datasets containing person-level and lesion-level variables. These datasets are utilized to summarize population-level measures, including age- and stage-specific incidence of bladder cancer, and lifetime risk of developing bladder cancer. The outputs are stratified by race, sex, and exposure status.

Output Listing

Figure 1 illustrates the structure of the primary datasets generated by the Kystis model. The person-level dataset includes demographic variables, birth date, cohort, and spawn age, which is the age at the beginning of the simulation. Exposure variables in the person-level dataset are limited to ever-exposed status. However, detailed smoking history can be obtained from the Smoking History Generator dataset linked by `person_id`, which provides information on smoking initiation age, smoking cessation age, and smoking intensity measured in cigarettes per day. The variable `toxin_ever_exposed` serves as a placeholder for occupational and environmental exposures that will be incorporated in future model releases. Variables representing the natural history include ages at two types of modeled symptoms (voiding symptoms and macroscopic bleeding), age and stage at clinical detection, and ages at various stages of bladder cancer (NMIBC, MIBC, metastasis). The person-level dataset also includes bladder cancer mortality and mortality from other causes, with `age_dead_all_causes` representing the minimum of these two.

The person-level and lesion-level datasets are linked by `person_id`. The lesion-level dataset is in a long format and includes variables related to lesions (`lesion_id`) and lesion transitions (`transition_id`). Lesion-level variables encompass the inception moment of the lesion, i.e., the date when the lesion appeared, and the persons's age at that moment, as well as lesion morphology. Each lesion transition is described with a state name, moment at state, and age at state on both the lesion's and persons's clock. Additionally, each state is categorized as precancerous lesion (`is_VLIP`), low-grade lesion (`is_HIP_LG`), non-muscle invasive bladder cancer (`is_NMIBS`), muscle invasive bladder cancer (`is_MIBS`), metastatic disease (`is_metastasis`), or the terminal state (`is_bcdeath`).

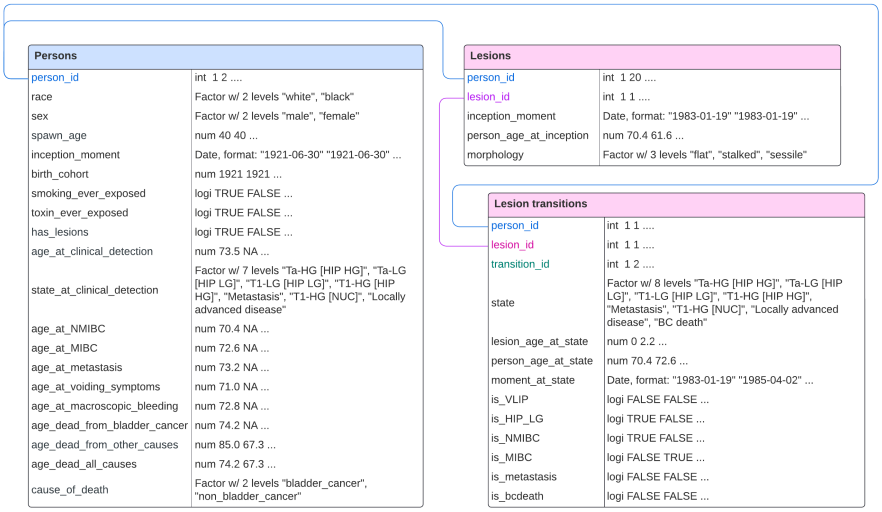

Figure 1. Bladder cancer natural history data sets in the *Kystis* model.

Population-level outputs include age- and stage-specific incidence of bladder cancer and lifetime risk of developing bladder cancer (Table 1).

Table 1. Population-level outputs in the `Kystis` model.

Output	Definition	Description
Age-specific incidence rate of bladder cancer per 100,000	$I_a = 10^5 \frac{C_a}{N_a}$	C_a is a number of people diagnosed with bladder cancer and N_a is a total population at risk in the age interval a. We use SEER 5-year age interval breaks starting from the age of 40, which is a spawn age in the model. Ages over 85 years are groupped as 85+ category.
Age-specific cumulative incidence rate of bladder cancer per 100,000, by stage	$I_{a,s} = 10^5 \frac{C_{a,s}}{N_{a,s}}$	$s \in \{$"NMIBS low grade", "NMIBS, high grade", "MIBS", "metastasis"$\}$.
Lifetime risk of developing bladder cancer	$LR = \sum_{a=0}^{K} I_a * S_a$	K is the allowed maximum age in the simulation, I_a is age-specific incidence of bladder cancer at age a, and S_a is a probability of surviving by age a.
Mean sojourn time	$ST = \frac{\sum_i D_i - O_i}{C}$	D_i is person's age of bladder cancer clinical detection, O_i is person's age at the first lesion inception moment, and C is a total number of people diagnosed with bladder cancer.

Results Overview

Summary

A guide to the results obtained from the model.

Overview

In the current version, we calibrated parameters of the natural history of bladder cancer for White Men, the population subgroup with the highest incidence of bladder cancer. We compared simulated data versus corresponding 2010 SEER estimates for a population-based simulation. We simulated the US population as stacked cohorts of people born between 1910 and 2010 (covering 0-100 years of age in 2010) with relative cohort sizes proportional to CENSUS data. We compared the simulated incidence in 5-year age groups (i.e., 40-44, 45-49, …, 80-84, 85+) with the corresponding age groups for the 2010 diagnosis year. The model was calibrated using EGO algorithm variant and BayCANN.[1,2]We used Latin-Hypercube sampling to generate design points and used the Poisson (pseudo)-likelihood as a calibration objective.

Additionaly, we examined how the calibrated model simulate key events, that are not directly observable in the data, such as tumor emergence, MIBC, and metastasis. We calculated age distributions at these events and the distributions of the time intervals between them for a cohort of White Men born in 1950.

Results

Figures 1 & 2 compare the simulated versus observed age- and stage-specific incidence of all bladder cancers at diagnosis in White Men for 2010. For almost all age- and stage-groups, the uncertainty intervals of the simulated and observed incidences overlap, indicating good agreement.

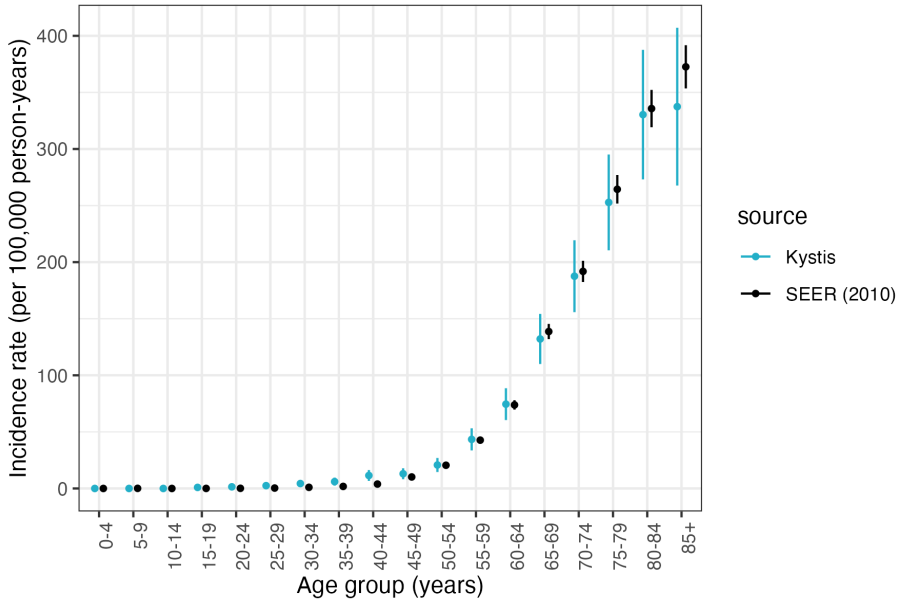

Figure 1. Age-specific bladder cancer incidence in White Men (U.S. in 2010).

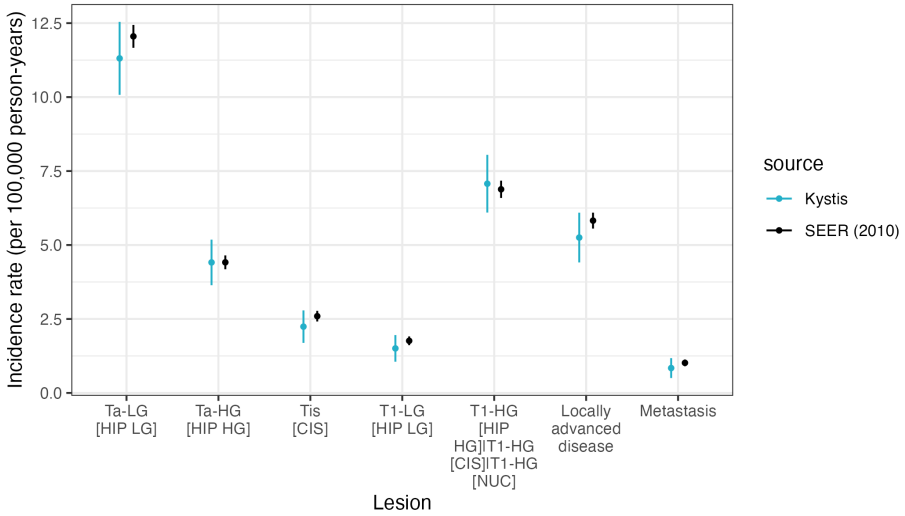

Figure 2. Stage-specific bladder cancer incidence in White Men (U.S. in 2010).

Figure 4 illustrates the lifetime risk of being diagnosed with bladder cancer. According to the model, individuals born in 1900 had an estimated lifetime risk of 2.0 percent. This risk gradually increased over time, following changes in life expectancy and smoking exposure. Estimates from Kystis indicate that lifetime risk peaked at 3.6 percent for those born between 1940 and 1950, then declined before rising again among the 1970 to 1980 birth cohorts.

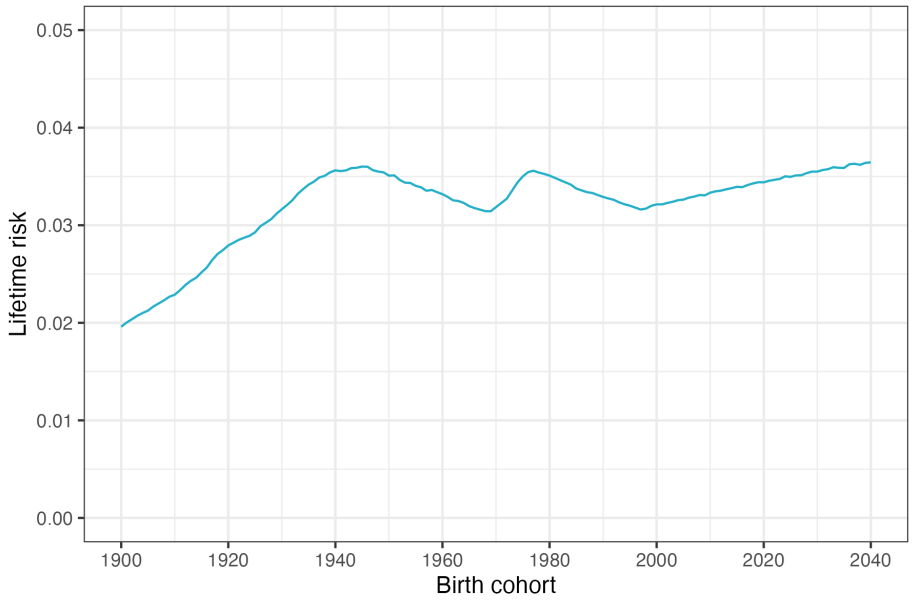

Figure 3. Bladder cancer lifetime risk in White Men (U.S., 1900-2040).

Figure 4a presents the predicted age-standardized incidence of bladder cancer from 2000 to 2040, using the US 2000 standard population as a reference. The model predictions align qualitatively with SEER data from 2000 to 2022, showing a slight decline in age-standardized incidence. SEER data indicates that incidence remained stable through 2004, followed by an annual decline of 1% from 2005 to 2022. `Kystis` estimates a more gradual decline of 0.6% per year between 2005 and 2021. The projected age-standardized incidence for 2040 is approximately 31.1 new cases per 100,000 person-years.

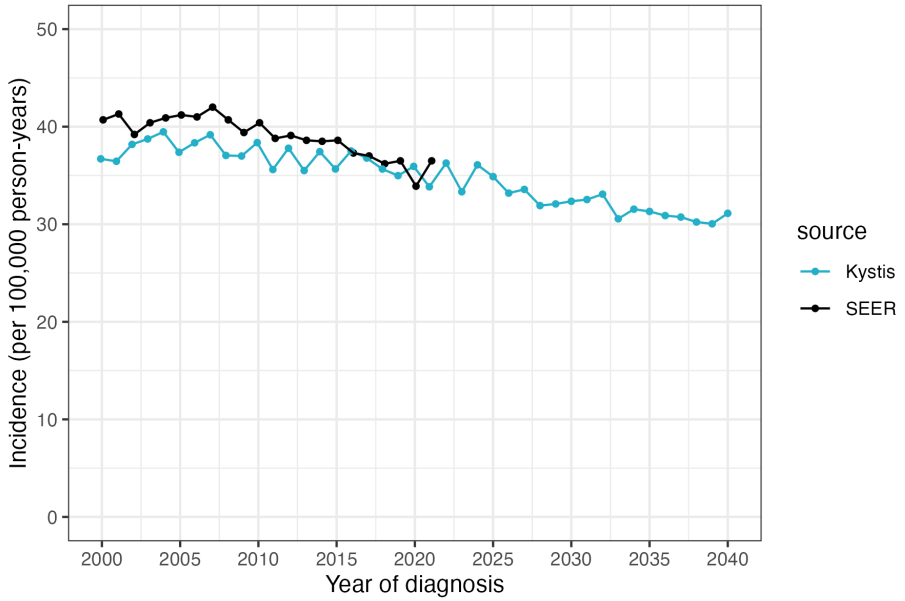

Figure 4a. Annual bladder cancer incidence in White Men (Age-adjusted estimates, U.S. 2000 standard population).

Projections of age-standardized incidence do not fully capture the expected changes in the population burden of bladder cancer. **Figure 4b** presents projections of the crude annual incidence of bladder cancer through 2040. According to `Kystis`, the annual incidence rate is expected to rise steadily from approximately 37 cases per 100,000 person-years in 2010 to around 45 cases per 100,000 person-years by 2040.

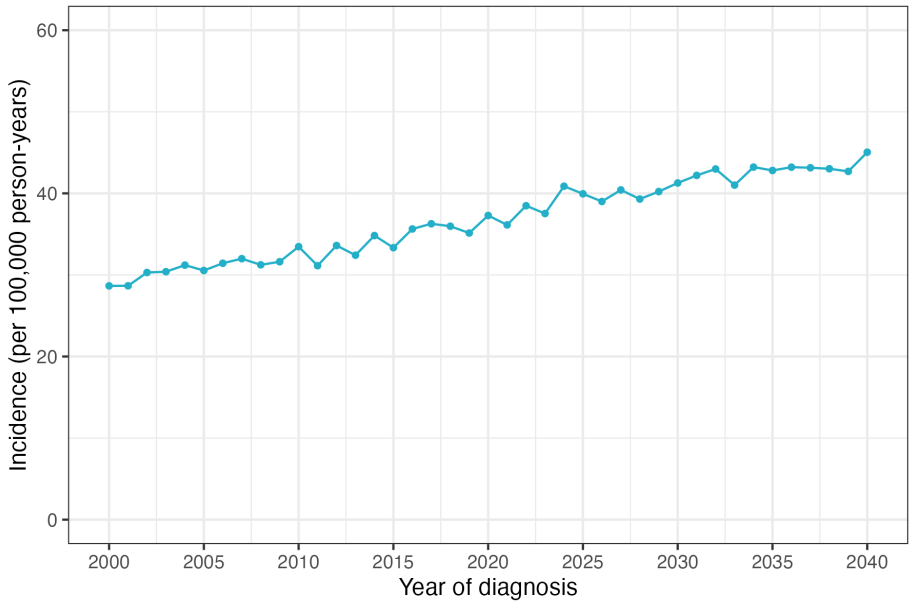

Figure 4b. Annual bladder cancer incidence in White Men (Crude estimates, U.S. population).

Figure 5 shows predicted annual prevalence of bladder cancer. According to the model, bladder cancer prevalence is slowly decreasing by approximately 0.1% per year on average.

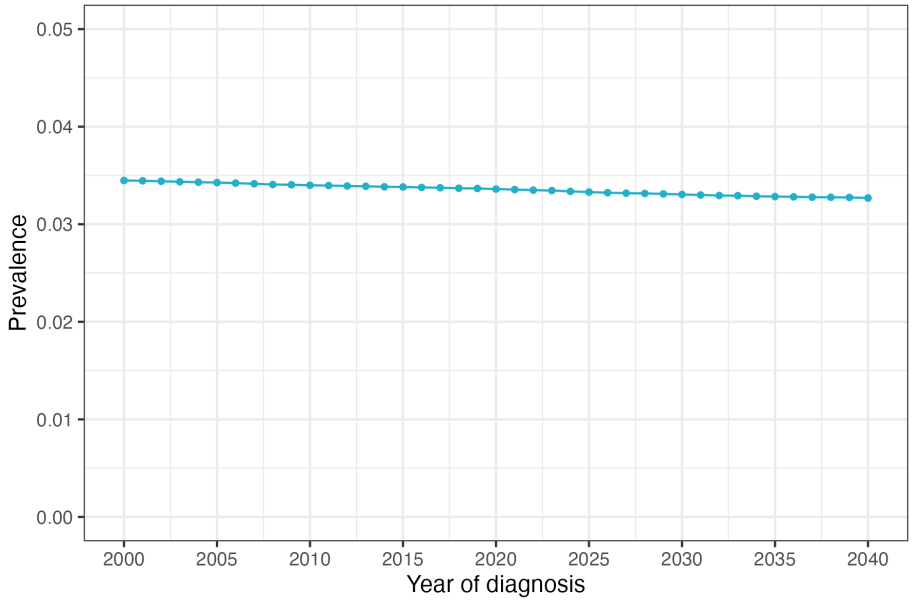

Figure 5. Annual bladder cancer prevalence in White Men (U.S. population).

Table 1 shows the median and 25-th and 75-th percentiles of the ages of key events in the natural history of bladder cancer as well as the time intervals between key events for the three models for White Men born in 1950. The median interval between the time when a lesion is detectable and diagnosis is about 3.3 years. The median time to MIBC from lesion emergence is about 2.7 years, and from MIBC to metastasis is about 1 year, with a wide distribution across simulated individuals.

Table 1. Ages of and time intervals between key events (White Men, 1950 cohort).

Description	Median (IQR)
Ages	
First lesion emergence	73.0 (63.7, 80.7)
Diagnosis	74.5 (65.7, 82.0)
MIBC	75.9 (67.1, 83.0)
Metastasis	76.4 (67.8, 83.6)
Time intervals, years	
Emergence to diagnosis	3.3 (2.7, 5.3)
Emergence to MIBC	2.7 (1.6, 4.4)
MIBC to metastasis	1.0 (0.4, 2.1)

References

1. Donald R Jones, Matthias Schonlau, William J Welch. Efficient global optimization of expensive black-box functions. Journal of Global optimization. Springer; 1998;13:455–492.
2. Hawre Jalal, Thomas A Trikalinos, Fernando Alarid-Escudero. BayCANN: streamlining Bayesian calibration with artificial neural network metamodeling. Frontiers in Physiology. Frontiers Media SA; 2021;12:662314.

BROWN

Key References

Elenir BC Avritscher, Catherine D Cooksley, H Barton Grossman, Anita L Sabichi, Lois Hamblin, Colin P Dinney, et al. Clinical Model of Lifetime Cost of Treating Bladder Cancer and Associated Complications. Urology. Elsevier; 2006;68(3):549–553.

Nicolas Bacaër. Verhulst and the logistic equation (1838). A short history of mathematical population dynamics. London: Springer London; 2011. p. 35–39.

Maximilian Burger, James WF Catto, Guido Dalbagni, H Barton Grossman, Harry Herr, Pierre Karakiewicz, et al. Epidemiology and Risk Factors of Urothelial Bladder Cancer. European Urology. Elsevier; 2013;63(2):234–241.

Marcus GK Cumberbatch, Ibrahim Jubber, Peter C Black, Francesco Esperto, Jonine D Figueroa, Ashish M Kamat, et al. Epidemiology of Bladder Cancer: A Systematic Review and Contemporary Update of Risk Factors in 2018. European Urology. Elsevier; 2018;74(6):784–795.

Marcus GK Cumberbatch, Aidan P Noon. Epidemiology, Aetiology and Screening of Bladder Cancer. Translational Andrology and Urology. AME Publications; 2019;8(1):5.

Jakub Dobruch, Siamak Daneshmand, Margit Fisch, Yair Lotan, Aidan P Noon, Matthew J Resnick, et al. Gender and Bladder Cancer: A Collaborative Review of Etiology, Biology, and Outcomes. European Urology. Elsevier; 2016;69(2):300–310.

Jonathan J Duplisea, Sharada Mokkapati, Devin Plote, Kimberly S Schluns, David J McConkey, Seppo Yla-Herttuala, et al. The development of interferon-based gene therapy for BCG unresponsive bladder cancer: from bench to bedside. World Journal of Urology. Springer; 2019;37:2041–2049.

Neal D Freedman, Debra T Silverman, Albert R Hollenbeck, Arthur Schatzkin, Christian C Abnet. Association between smoking and risk of bladder cancer among men and women. Jama. American Medical Association; 2011;306(7):737–745.

Petrisor Aurelian Geavlete. Endoscopic Diagnosis and Treatment in Urinary Bladder Pathology: Handbook of Endourology. Academic Press; 2016.

Dharmesh Gopalakrishnan, Vadim S Koshkin, Moshe C Ornstein, Athanasios Papatsoris, Petros Grivas. Immune Checkpoint Inhibitors in Urothelial Cancer: Recent Updates and Future Outlook. Therapeutics and Clinical Risk Management. Taylor & Francis; 2018;14:1019–1040.

International Organization for Standardization. International Standard for the Representation of Dates and Times: ISO 8601 [Internet]. 2020. Available from: https://www.iso.org/iso-8601-date-and-time-format.html

Hawre Jalal, Thomas A Trikalinos, Fernando Alarid-Escudero. BayCANN: streamlining Bayesian calibration with artificial neural network metamodeling. Frontiers in Physiology. Frontiers Media SA; 2021;12:662314.

Jihyoun Jeon, Rafael Meza, Martin Krapcho, Lauren D Clarke, Jeff Byrne, David T Levy. Chapter 5: Actual and counterfactual smoking prevalence rates in the US population via microsimulation. Risk Analysis: An International Journal. Wiley Online Library; 2012;32:S51–S68.

Donald R Jones, Matthias Schonlau, William J Welch. Efficient global optimization of expensive black-box functions. Journal of Global optimization. Springer; 1998;13:455–492.

Jack PC Kleijnen. Antithetic variates, common random numbers and optimal computer time allocation in simulation. Management Science. INFORMS; 1975;21(10):1176–1185.

Pierre L'Ecuyer, Christian Lécot, Bruno Tuffin. A randomized quasi-Monte Carlo simulation method for Markov chains. Operations research. INFORMS; 2008;56(4):958–975.

Virginia A Moyer. Screening for bladder cancer: US Preventive Services Task Force recommendation statement. Annals of internal medicine. American College of Physicians; 2011;155(4):246–251.

NCI. SEER Cancer Stat Facts: Bladder Cancer 2019 [Internet]. 2019. Available from: https://seer.cancer.gov/statfacts/html/urinb.html

Cyrill A Rentsch, Claire Biot, Joël R Gsponer, Alexander Bachmann, Matthew L Albert, Romulus Breban. BCG-Mediated Bladder Cancer Immunotherapy: Identifying Determinants of Treatment Response Using a Calibrated Mathematical Model. PloS one. 2013 Feb;8(2):e56327-17.

Rebecca L Siegel, Kimberly D Miller, Hannah E Fuchs, Ahmedin Jemal. Cancer Statistics, 2022. CA: A Cancer Journal for Clinicians. 2022;72(1).

John A Spratt, D Von Fournier, John S Spratt, Ernst E Weber. Decelerating growth and human breast cancer. Cancer. Wiley Online Library; 1993;71(6):2013–2019.

Robert S Svatek, Brent K Hollenbeck, Sten Holmäng, Richard Lee, Simon P Kim, Arnulf Stenzl, et al. The Economics of Bladder Cancer: Costs and Considerations of Caring for This Disease. European Urology. Elsevier; 2014;66(2):253–262.

Thomas A Trikalinos, Yuliia Sereda. The nhppp package for simulating non-homogeneous Poisson point processes in R. PLoS One. Public Library of Science San Francisco, CA USA; 2024;19(11):e0311311.

Thomas A Trikalinos, Yuliia Sereda. nhppp: Simulating Nonhomogeneous Poisson Point Processes in R. arXiv preprint arXiv:240200358. 2024;

Panagiotis J Vlachostergios, Christopher D Jakubowski, Muhammad J Niaz, Aileen Lee, Charlene Thomas, Amy L Hackett, et al. Antibody-drug conjugates in bladder cancer. Bladder Cancer. IOS Press; 2018;4(3):247–259.

Yu Wang, Qian Chang, Yang Li. Racial differences in urinary bladder cancer in the United States. Scientific Reports. Nature Publishing Group UK London; 2018;8(1):12521.

Adam B Weiner, Mary-Kate Keeter, Adarsh Manjunath, Joshua J Meeks. Discrepancies in staging, treatment, and delays to treatment may explain disparities in bladder cancer outcomes: an update from the National Cancer Data Base (2004–2013). Urologic Oncology: Seminars and Original Investigations. Elsevier; 2018. p. 237-e9.

John R Wilmoth, Kirill Andreev, Dmitri Jdanov, Dana A Glei, C Boe, M Bubenheim, et al. Methods protocol for the human mortality database. University of California, Berkeley, and Max Planck Institute for Demographic Research, Rostock URL: http://mortality org [version 31/05/2007]. 2007;9:10–11.

Wesley Yip, Giovanni Cacciamani, Sumeet K Bhanvadia. Disparities in bladder cancer outcomes based on key sociodemographic characteristics. Current Urology Reports. Springer; 2020;21:1–6.

Columbia University
Version: 1.0.00
Released: 2025-09-30

Simulation of Cancers of the Urinary Tract (SCOUT): Model Profile

Columbia University Irving Medical Center

Contact

Stella Kang (sk5603@cumc.columbia.edu)

Suggested Citation

Siriruchatanon M, Gu Z, Huang W, Kang SK. Simulation of Cancers of the Urinary Tract (SCOUT): Model Profile. [Internet] Sep 30, 2025. Cancer Intervention and Surveillance Modeling Network (CISNET). Available from: https://cisnet.cancer.gov/resources/files/mpd/bladder/CISNET-bladder-scout-model-profile-1.0.00-2025-09-30.pdf

Version Table

Version	Date	Notes
1.0.00	2025-09-30	Initial release

Columbia University
Readers Guide

Reader's Guide

Core Profile Documentation

These topics will provide an overview of the model without the burden of detail. Each can be read in about 5-10 minutes. Each contains links to more detailed information if required.

Model Purpose
This document describes the primary purpose of the model.

Model Overview
This document describes the primary aims and general purposes of this modeling effort.

Assumption Overview
An overview of the basic assumptions inherent in this model.

Parameter Overview
Describes the basic parameter set used to inform the model, more detailed information is available for each specific parameter.

Component Overview
A description of the basic computational building blocks (components) of the model.

Output Overview
Definitions and methodologies for the basic model outputs.

Results Overview
A guide to the results obtained from the model.

Key References
A list of references used in the development of the model.

Model Purpose

Summary

This document describes in broad strokes the purpose for the development of the Simulation of Cancers of the Urinary Tract (SCOUT) Model.

Purpose

The prevalence of chronic kidney disease (CKD) is high among older adults,[1] persons with hypertension,[2] and/or those with diabetes.[2] In turn, CKD is associated with increased risk of cardiovascular mortality [3] and also mortality related to specific cancers.[4,5]Specifically, the urinary tract (kidney, ureters, bladder) is the source of the second-most common cause of cancer deaths in this population.[4] CKD and smoking are independently associated with the risk of urinary tract cancer, including bladder cancer.[6,7]SCOUT incorporates major risk factors and comorbid conditions contributing to the risk of bladder cancer, cancer-specific mortality risk, and other competing mortality risks. By incorporating risk categories defined by individual characteristics and risk factors, SCOUT is enabled for assessing the comparative effectiveness of screening and management strategies for bladder cancer in both the general population as well as specific populations with higher incidence of bladder cancers.

The purpose of the SCOUT model can be summarized in four aims:

1. Simulate a hypothetical population of individuals with and without CKD with broad-ranging risk for urinary system cancers and competing mortality risks
2. Simulate bladder cancer incidence and mortality in individuals with and without CKD according to the nationally representative data
3. Incorporate bladder cancer treatment pathways according to the clinical guidelines along with post-treatment events
4. Identify whether circumstances exist under which benefits outweigh the harms of urinary system cancer screening in the general population or in subpopulations with elevated risk of bladder cancer

References

1. United States Renal Data System. 2023 USRDS Annual Data Report: Epidemiology of kidney disease in the United States [Internet]. 2023. Available from: https://adr.usrds.org/2023
2. A. X. Garg, B. A. Kiberd, W. F. Clark, R. B. Haynes, C. M. Clase. Albuminuria and renal insufficiency prevalence guides population screening: results from the NHANES III. Kidney Int. 2002;61(6):2165–75.
3. A. S. Go, G. M. Chertow, D. Fan, C. E. McCulloch, C. Y. Hsu. Chronic kidney disease and the risks of death, cardiovascular events, and hospitalization. N Engl J Med. 2004;351(13):1296–305.
4. S. D. Navaneethan, J. D. Schold, S. Arrigain, S. E. Jolly, Jr. Nally J. V. Cause-Specific Deaths in Non-Dialysis-Dependent CKD. J Am Soc Nephrol. 2015;26(10):2512–20.
5. A. Christensson, C. Savage, D. D. Sjoberg, A. M. Cronin, M. F. O'Brien, W. Lowrance, et al. Association of cancer with moderately impaired renal function at baseline in a large, representative, population-based cohort followed for up to 30 years. Int J Cancer. 2013;133(6):1452–8.
6. W. T. Lowrance, J. Ordonez, N. Udaltsova, P. Russo, A. S. Go. CKD and the risk of incident cancer. J Am Soc Nephrol. 2014;25(10):2327–34.
7. N. D. Freedman, D. T. Silverman, A. R. Hollenbeck, A. Schatzkin, C. C. Abnet. Association between smoking and risk of bladder cancer among men and women. JAMA. 2011;306(7):737–45.

Columbia University
Model Overview

COLUMBIA UNIVERSITY

Model Overview

Summary

This document provides a summary of the Simulation of Cancers of the Urinary Tract (SCOUT) model. SCOUT is a microsimulation model that simulates a hypothetical cohort with established risk factors for bladder cancers such as chronic kidney disease, smoking, and hypertension.

Purpose

The SCOUT model is developed to assess the comparative effectiveness of screening in general and specific populations for bladder cancers, while accounting for major risk factors including CKD severity, smoking, sex, age, and race. See Model Purpose for more details.

Background

Chronic kidney disease (CKD) is a prevalent condition that is associated with multiple other disease, including cancer. The prevalence of CKD is approximately 14% among U.S. adults overall and 33.2% among older adults (≥65 years).[1] Persons with CKD are at risk for early mortality compared to those with normal kidney function. According to a retrospective cohort study using the third National Health and Nutrition Examination Survey, the 10-year cumulative cardiovascular mortality rate was 9.9% (95% CI: 7.9–11.9%) among individuals with kidney disease, compared to 3.4% (95% CI: 3.1–3.7%) among healthy individuals.[2] Furthermore, a recent systematic review and meta-analysis reported that persons with CKD are 1.35 times more likely to develop urothelial cancers compared to those with preserved kidney function.[3]

Among the types of urinary tract cancers, bladder cancers have the highest incidence. In 2023, an estimated 82,290 of new cases of bladder cancer were diagnosed making it the sixth highest incident cancer in the US.[4] Moreover, urinary bladder cancers were the eighth most common cause of cancer-specific deaths in 2023 resulting in an estimated 16,710 deaths.[4] Despite the significant burden of bladder cancer and the availability of increasingly accurate detection tests, there are currently no recommendations for urinary tract cancer screening programs. Use of microsimulation modeling can serve as a valuable tool for addressing health policy questions regarding risk-based urinary bladder screening approaches among high-risk individuals such as persons with CKD, where early stage disease is crucial for the greatest chance at effective therapy. This decision-analytic tool can be applied to the design and guidance of randomized controlled trials as new technologies and risk information are available, aiming to improve in early-stage diagnosis and treatment.

Model Description

The SCOUT model is a discrete-time non-homogenous Markov microsimulation model. Our model simulates persons with various risk factors and comorbidities relevant to risk of urinary tract cancer including sex, tobacco smoking status, diabetes mellitus, hypertension, and CKD. SCOUT first initiates a hypothetical cohort of the same sex and race at the age of 30 with individual risk factors. A simulated person receives a static risk factor of smoking status (Never, Former, Current) and time-varying risk factors of diabetes mellitus, hypertension, and CKD. Specifically, each person may develop diabetes and/or hypertension over their lifetime, which further influences the development and progression of CKD and bladder cancer (**Figure 1**). SCOUT is written in Python.

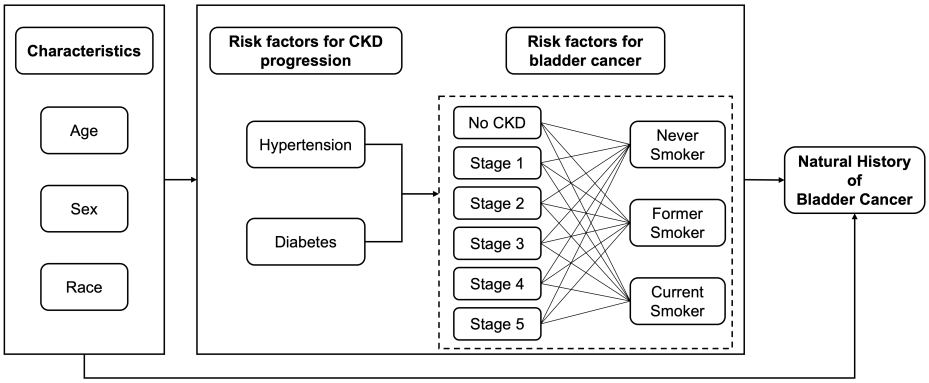

Figure 1. Individual characteristics and risk factors associated with CKD progression and natural history of bladder cancer in the SCOUT model.

SCOUT consists of 4 components:

1. Chronic kidney disease development and progression
2. Natural history of bladder cancer
3. Screening (in development)
4. Treatment and surveillance (in development)

Chronic kidney disease

SCOUT simulates the development and progression of CKD with seven stages (no CKD, stage 1, stage 2, stage 3a, stage 3b, stage 4, stage 5) using a yearly cycle. The CKD stage is defined by glomerular filtration rate (GFR) and albuminuria categories (normal, microalbuminuria, macroalbuminuria) according to Kidney Diseases: Improving global Outcomes (KDIGO).[5] At the beginning of the time horizon, each simulated person is assigned diabetes and/or hypertension status (presence or absence), GFR, and albuminuria level of normal or micro-albuminuria. At each cycle, a person may develop hypertension and/or diabetes, experience a decline in GFR, develop micro-albuminuria or have a transition from micro- to macro-albuminuria. The rates of GFR decline, incidence rates of microalbuminuria, and the transition probability from micro- to macroalbuminuria depends on age, sex, and presence/absence of hypertension and diabetes.[6-8]A person with CKD progresses in increasing severity of CKD stages. The severity of CKD stages further informs the risk of bladder cancer, non-cardiovascular disease (CVD) and CVD mortality risk. The CKD component was calibrated to the prevalence of CKD and incidence of end-stage renal disease obtained from the United States Renal Data System (USRDS) report.[1] See Chronic Kidney Disease component for more details.

Natural history of bladder cancer

SCOUT simulates the development and progression of bladder cancers with four main health states: disease-free, non-muscle invasive bladder cancers or NMIBC (Ta, Tis, T1), muscle invasive bladder cancers or MIBC (T2, T3, T4 excluding metastatic disease), and metastasis using a monthly cycle. At the beginning of the time horizon, each simulated person is assigned established risk factors associated with bladder cancer including static smoking status, and CKD stage as described in the CKD component. At each cycle, a person may experience one of the following: remain tumor-free, develop low-grade Ta or high-grade Ta that is initially undetectable (presence of tumor without detectable clinical signs or symptoms), transition from undetectable to detectable state (with clinical signs or symptoms) for those with NMIBC, transition from detectable to detected stage (for those with NMIBC), transition from low to high grade (for those with NMIBC), and experience an increase in T stage. The probability of developing tumors depends on age, sex, smoking status, and CKD stage. For those with bladder tumors, SCOUT applied the probability transitioning from less severe to more severe health states depending on age and sex. All probabilities applied to the model are updated monthly and are conditional probabilities depending only on the health state from the previous month. Once a person reach metastasis, they are subject to metastatic death in addition to other causes of death including non-CVD and CVD. The natural history of bladder cancer was first calibrated to SEER observed cancer incidence for white men, given the predominance of bladder cancer diagnoses occurring in this population. See Natural history of bladder cancer component for more details.

References

1. United States Renal Data System. 2023 USRDS Annual Data Report: Epidemiology of kidney disease in the United States [Internet]. 2023. Available from: https://adr.usrds.org/2023
2. M. Afkarian, M. C. Sachs, B. Kestenbaum, I. B. Hirsch, K. R. Tuttle, J. Hinnmelfarb, et al. Kidney Disease and Increased Mortality Risk in Type 2 Diabetes. Journal of the American Society of Nephrology. 2013;24(2):302–308.
3. Emily R Brooks, Mutita Siriruchatanon, Vinay Prabhu, David M Charytan, William C Huang, Yu Chen, et al. Chronic kidney disease and risk of kidney or urothelial malignancy: systematic review and meta-analysis. Nephrology Dialysis Transplantation. 2023;
4. R. L. Siegel, K. D. Miller, N. S. Wagle, A. Jemal. Cancer statistics, 2023. CA Cancer Journal for Clinicians. 2023;73(1):17–48.
5. A. Levin, P. E. Stevens. Summary of KDIGO 2012 CKD Guideline: behind the scenes, need for guidance, and a framework for moving forward. Kidney Int. 2014;85(1):49–61.
6. L. E. Boulware, B. G. Jaar, M. E. Tarver-Carr, F. L. Brancati, N. R. Powe. Screening for proteinuria in US adults: a cost-effectiveness analysis. JAMA. 2003;290(23):3101–14.
7. B. O. Yarnoff, T. J. Hoerger, S. S. Shrestha, S. K. Simpson, N. R. Burrows, A. H. Anderson, et al. Modeling the impact of obesity on the lifetime risk of chronic kidney disease in the United States using updated estimates of GFR progression from the CRIC study. PLoS One. 2018;13(10):e0205530.
8. T. J. Hoerger, J. S. Wittenborn, J. E. Segel, N. R. Burrows, K. Imai, P. Eggers, et al. A health policy model of CKD: 1. Model construction, assumptions, and validation of health consequences. Am J Kidney Dis. 2010;55(3):452–62.

Assumption Overview

Summary

An overview of the basic assumptions inherent in this model. This document briefly describes the assumptions made by the Simulation of Cancers of the Urinary Tract (SCOUT) model.

Background

To create a microsimulation model, assumptions are required to simplify the complexity of disease progression.

Assumption Listing

Model assumptions are listed for each component of the SCOUT model.

Chronic kidney disease

- Initial distribution of GFR for adults of age 30 years follows the truncated normal distribution.
- Systolic blood pressure by age, sex, and CKD status is assumed to follow a distribution based on percentile rank values derived from NHANES III.
- For adults of age 30, the prevalence of diabetes and microalbuminuria is assumed to be zero.
- Albumin-to-creatinine ratio (ACR) is assumed to be the only marker of kidney damage in the current version of SCOUT. Other markers such as urine sediment abnormalities, history of kidney transplant, or electrolyte and other abnormalities due to tubular disorders are excluded from the model.
- The annual rate of decline in GFR is assumed to be heterogeneous among the simulated cohort with the same risk factors, achieved by applying an individual coefficient multiplier following a symmetric triangular distribution.
- Higher rates of CKD progression are applied to persons who develop diabetes and/or hypertension after a duration of two cycles.
- The mortality rate for end-stage renal disease is applied to persons who reach CKD stage 5 after a duration of one cycle.

Natural history of bladder cancer

- The undetectable tumor state refers to a presence of bladder cancer tumor without any sign of symptoms.
- The detectable tumor state refers to bladder cancer tumor that exhibits common symptoms such as microscopic or macroscopic hematuria.
- The detected tumor state refers to any bladder cancer tumors that are clinically diagnosed.
- Any muscle invasive bladder cancers (MIBC T2-T4 excluding metastatic disease) are assumed to be symptomatic and detectable.
- For each of the T stages among MIBC, we assumed a proportion of these tumors are detected, where a higher proportion of tumors is detected in more severe T stages.
- We assumed the transition time from undetectable to detectable TaHG is no longer than 1.5 years.[1] Consequently, the transition time from undetectable to detectable TaLG is assumed to be longer than that of TaHG, while the transitioning time for T1 is assumed to be shorter.[2-6]
- The probability of developing a bladder tumor and the probability of transitioning between T stages increase with age.

References

1. H. Calkins, Y. Shyr, H. Frumin, A. Schork, F. Morady. The value of the clinical history in the differentiation of syncope due to ventricular tachycardia, atrioventricular block, and neurocardiogenic

syncope. Am J Med. 1995;98(4):365–73.
2. Y. Lotan, K. Elias, R. S. Svatek, A. Bagrodia, G. Nuss, B. Moran, et al. Bladder cancer screening in a high risk asymptomatic population using a point of care urine based protein tumor marker. J Urol. 2009;182(1):52–7; discussion 58.
3. E. M. Messing, T. B. Young, V. B. Hunt, E. B. Roecker, A. M. Vaillancourt, W. J. Hisgen, et al. Home screening for hematuria: results of a multiclinic study. J Urol. 1992;148(2 Pt 1):289–92.
4. E. M. Messing, T. B. Young, V. B. Hunt, J. M. Wehbie, P. Rust. Urinary tract cancers found by homescreening with hematuria dipsticks in healthy men over 50 years of age. Cancer. 1989;64(11):2361–7.
5. E. M. Messing, T. B. Young, V. B. Hunt, K. W. Gilchrist, M. A. Newton, L. L. Bram, et al. Comparison of bladder cancer outcome in men undergoing hematuria home screening versus those with standard clinical presentations. Urology. 1995;45(3):387–96; discussion 396-7.
6. E. M. Messing, T. B. Young, V. B. Hunt, M. A. Newton, L. L. Bram, A. Vaillancourt, et al. Hematuria home screening: repeat testing results. J Urol. 1995;154(1):57–61.

Parameter Overview

Summary

This document provides the parameters used in the Simulation of Cancers of the Urinary Tract (SCOUT) model.

Background

Parameters in the SCOUT model are informed by systematic review, observational data from the literature or nationally representative datasets. Any unknow parameters are calibrated to the targets derived from U.S. observed data.

Parameter Listing Overview

Parameters are listed for each component of the SCOUT model.

Chronic kidney disease

1. Incidence rate of diabetes by age, sex, and race
2. Incidence rate of micro-albuminuria by age, sex, race, and diabetes and hypertension status
3. Initial systolic blood pressure for middle-aged adults
4. Change in systolic blood pressure by age, sex, and presence/absence of CKD
5. Annual rate of decline in GFR by level of GFR, presence of macroalbuminuria, diabetes status, and hypertension status
6. Annual transition probability from micro- to macro-albuminuria by age, sex, diabetes status, and hypertension status
7. Hazard ratios of non-CVD and CVD mortality risk for those with CKD compared to those without CKD stratified by CKD stage
8. CVD mortality rates by age, sex, and race
9. Background mortality rate by age, sex, and race
10. Mortality rates among people with end-stage renal disease by age, sex, race, diabetes status, and hypertension status

Natural history of bladder cancer

1. Prevalence of smoking status in adults age ≥ 40 by sex
2. Proportion of hematuria among non-muscle invasive bladder cancer
3. Probability of developing undetectable low-grade papillary tumor (TaLG) by age, sex, smoking status, and CKD severity
4. Probability of developing undetectable high-grade papillary tumor (TaHG) by age, sex, smoking status, and CKD severity
5. Probability of transitioning from undetectable TaLG to detectable TaLG
6. Probability of transitioning from undetectable TaLG to undetectable TaHG/Tis
7. Probability of transitioning from undetectable TaLG to detectable TaHG/Tis
8. Probability of transitioning from detectable TaLG to detectable TaHG/Tis
9. Probability of transitioning from undetectable TaHG/Tis to detectable TaHG/Tis
10. Probability of transitioning from undetectable TaHG/Tis to undetectable T1 by age
11. Probability of transitioning from undetectable TaHG/Tis to detectable T1 by age
12. Probability of transitioning from detectable TaHG/Tis to detectable T1 by age
13. Probability of transitioning from undetectable T1 to detectable T1
14. Probability of transitioning from undetectable T1 to T2 by age
15. Probability of transitioning from T2 to T3 by age
16. Probability of transitioning from T3 to T4
17. Probability of transitioning from T4 to metastasis

18. Rate of detection of detectable TaLG
19. Rate of detection of detectable TaHG
20. Rate of detection of detectable T1
21. Proportion of tumor detected in MIBC by T stage, age, and sex
22. Probability of death from metastatic bladder cancer
23. Hazard ratios of risk of bladder cancer for those with severe CKD stage compared to those without CKD
24. Hazard ratios of risk of bladder cancer for former/current smokers compared to non-smokers
25. Hazard ratios of non-CVD and CVD mortality risk for those with CKD compared to those without CKD stratified by CKD stage
26. CVD mortality rates by age, sex, and race
27. Mortality rates among people with end-stage renal disease by age, sex, race, diabetes status, and hypertension status
28. Background mortality rate by age, sex, and race

Component Overview

Summary

This document provides the overview of major components of the Simulation of Cancers of the Urinary Tract (SCOUT) model.

Overview

SCOUT consists of four major components: 1) Chronic kidney disease, 2) Natural history of bladder cancer, 3) Screening (in development), and 4) Treatment and surveillance (in development). All components are designed to run simultaneously by default. However, the chronic kidney disease and the natural history components can be run independently. Consequently, SCOUT can simulate a cohort with CKD progression and without cancer progression. Similarly, a cohort with only cancer progression can be simulated as needed.

Component Listing

Chronic Kidney Disease

The Chronic Kidney Disease component simulates a hypothetical cohort of individuals with the same sex, age, and race who may develop diabetes and/or hypertension over time. These comorbid conditions influence the rate of CKD progression. The CKD component models the progression from no CKD to CKD stages 1 through 5. The severity of CKD stages further informs the risk of bladder cancer, as well as non-CVD and CVD mortality risk. Additionally, SCOUT can simulate a cohort with the same initial CKD stage as well.

Natural history of bladder cancer

By default, the Natural History component is developed to run simultaneously with the CKD component, accounting for individual changes in CKD severity in addition to the static smoking status. The smoking status is initialized based on the prevalence of smoking among U.S. adults from age 40, obtained from a national dataset. In the current version of SCOUT, smoking status is assigned at the start of the model and is independent of CKD and, therefore, does not influence CKD progression. The natural history component simulates the progression of bladder cancers, from a disease-free state to the development of bladder tumors, ranging from non-muscle invasive bladder cancers, muscle invasive bladder cancers, and metastasis. All simulated individuals are subject to non-CVD and CVD mortality risks, with varying risks based on CKD severity. Only those with metastasis are subject to death from metastatic disease. Additionally, the natural history of bladder cancer component can be run independent of CKD component as well.

Output Overview

Summary

This document provides an overview of outputs generated from the Simulation of Cancers of the Urinary Tract (SCOUT) model.

Overview

SCOUT tracks individual trajectories of characteristics, risk factors, cancer stage, time to cancer development, time of progression between cancer stages, time of death, and causes of death over a lifetime. Accordingly, SCOUT can generate the outputs for the overall simulated cohort and for sub-cohorts based risk factors and comorbidities.

Output Listing

The model outcomes are generated using a lifetime horizon and can be stratified by smoking status and/or CKD stage. The main outputs include:

- Age- and stage-specific bladder cancer incidence
- Mean age at diagnosis
- Cumulative cancer mortality
- Cumulative all-cause mortality
- Cumulative CVD mortality
- Cumulative end-stage renal disease mortality
- Prevalence of CKD by age group
- Cumulative incidence of end-stage renal disease
- Life expectancy

Additional outputs will be provided when the screening and treatment components are completed.

Columbia University
Results Overview

COLUMBIA UNIVERSITY

Results Overview

Summary

This document provides is a summary of the model results from developing the Simulation of Cancers of the Urinary Tract (SCOUT) model and its application.

Overview

SCOUT is a microsimulation following a discrete-time non-homogeneous Markov model. In the current version, we developed and calibrated our model for two components: chronic kidney disease and natural history of bladder cancer. For the chronic kidney disease component, we calibrated the parameter relevant to CKD progression using grid search. Most of our model targets fall within the USRDS reported ranges of prevalence of CKD by age and the cumulative incidence of end-stage renal disease. Lastly, we applied the calibrated parameters relevant to CKD and calibrated the parameters relevant to bladder cancer development and progression. The natural history model was calibrated using incremental mixture approximate Bayesian computation. Our model outcomes match well with the age-specific cancer incidence and stage-specific cancer incidence derived from SEER Cancer registry for white men (Figure 1 and 2).

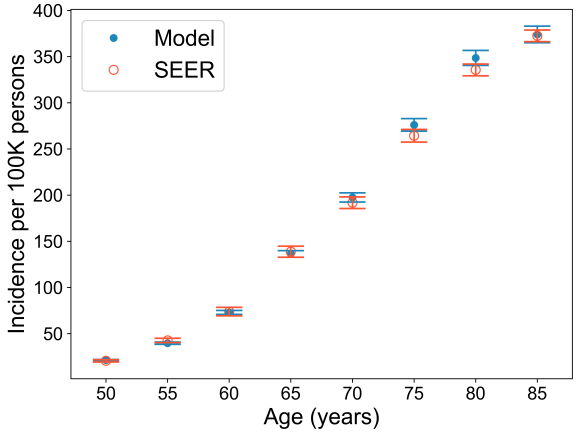

Figure 1. Model calibration for age-specific incidence comparing SCORE against SEER for white men diagnosed in 2010

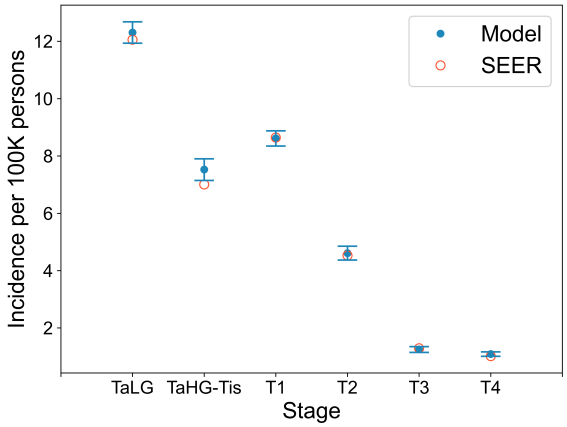

Figure 2. Model calibration for stge-specific incidence comparing SCORE against SEER for white men diagnosed in 2010

Results List

Model results in detail will be updated as a list of publications associated with brief description.

Columbia University
CKD Component

COLUMBIA UNIVERSITY

CKD Component

Summary

This document describes the development and disease progression of chronic kidney disease (CKD) of the Simulation of Cancers of the Urinary Tract (SCOUT) model.

Overview

The chronic kidney disease component of SCOUT simulates CKD development and its progression to end-stage renal disease based on a decline in glomerular filtration rate and the development of micro- and macroalbuminuria. Additionally, SCOUT incorporate risk factors associated with CKD by simulating the incidence of diabetes and changes in systolic blood pressure, indicating the presence of hypertension.

Details

SCOUT simulates the development and progression of CKD with seven stages: no CKD, stage 1, stage 2, stage 3a, stage 3b, stage 4, stage 5 (Table 1) using a yearly cycle. Following KDIGO 2012,[1] we categorize CKD stage based on six levels of glomerular filtration rate (GFR) and three albuminuria categories (normal, microalbuminuria, macroalbuminuria). SCOUT incorporated risk factors associated with the risk of CKD including age, sex, race, and two comorbid conditions: hypertension and diabetes (presence/absence). At the beginning of the time horizon, SCOUT simulates a hypothetical cohort of the same sex, age, and race. Each person is assigned GFR level (continuous variable following truncated normal distribution), either having normal or microalbuminuria, presence or absence of diabetes, and level of systolic blood pressure (SBP). Hypertension is defined as SBP > 140 mmHg. At each cycle, SCOUT tracks individual change in diabetes status and SBP level, which further affect rates of progression in CKD stage.

For persons without CKD, they may develop CKD through one of the two pathways: 1) the onset of microalbuminuria, defined as kidney damage or an albumin-to-creatinine ratio (ACR) ≥ 30 mg/g or 2) a decrease in GFR to < 60 mL/min/1.73m^2 (Figure 1). For persons who initially have normal albuminuria but later develop microalbuminuria with GFR ≥ 60 mL/min/1.73m^2, they may transition from a no-CKD state to either CKD stage 1 or stage 2 depending on their GFR levels. The microalbuminuria incidence rate depends on age, sex, race, and the presence/absence of diabetes and hypertension. During their lifetime, persons with microalbuminuria may progress to have macroalbuminuria. For those with a decreased GFR < 60 mL/min/1.73m^2 and without microalbuminuria, the transition occurs directly from a no-CKD state to CKD stage 3a. For those with CKD, they may transition to more severe stages of CKD ranging from stage 1 to stage 5. The rates of transitioning are informed by 1) an annual rate of decline in GFR, 2) the incidence rate of microalbuminuria, and 3) a transition probability from micro- to macroalbuminuria. SCOUT models heterogenous declines in GFR among a simulated cohort with the same risk factors by applying a small adjustment to the rate of decline. To adjust the decline rate, each person receives a coefficient multiplier sampling from the symmetric triangular distribution. Compared to those without macroalbuminuria, those with macroalbuminuria are subject to higher rates of GFR decline. Additionally, those with comorbidity are subject to higher rates of GFR decline, microalbuminuria incidence rates, and probability of transitioning from micro- to macroalbuminuria. From any alive state, a person may die from various causes of death including CVD and non-CVD mortality. CVD and non-CVD mortality rates are higher in persons with more severe CKD stages. For persons with CKD stage 5, they are subject to the mortality rate of end-stage renal disease only. Over the time horizon, SCOUT tracks individual trajectories of age, GFR, SBP, albuminuria category, diabetes status, hypertension status, and CKD stage. See Parameter Overview and Assumption Overview for more details.

Table 1. CKD stage defined by albuminuria and glomerular filtration rate (GFR).

CKD Stage	Albuminuria category	GFR
No CKD	Normal	60+

CKD Stage	Albuminuria category	GFR
1	Microalbuminuria or Macroalbuminuria	90+
2	Microalbuminuria or Macroalbuminuria	60-89
3a	Any	45-60
3b	Any	30-45
4	Any	15-30
5	Any	<15

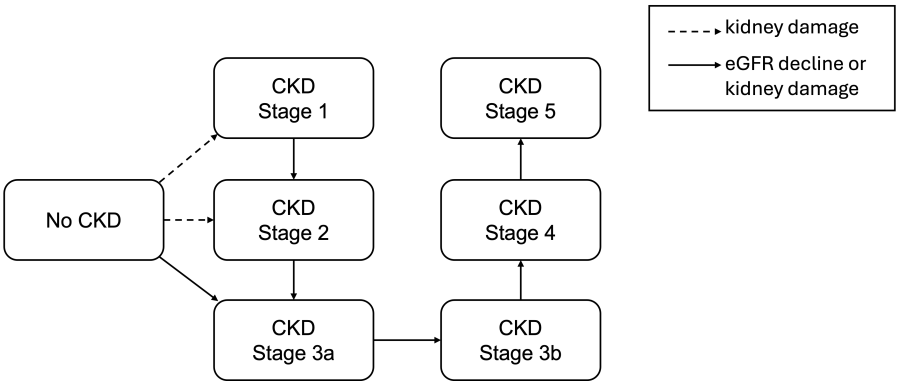

Figure 1. Chronic kidney disease development and progression.

To align with the U.S. observed data, we calibrated the CKD component for men to targets derived from the USRDS 2023 Annual Report.[2] The targets include the prevalence of CKD by age, the cumulative incidence of end-stage renal disease, the prevalence of CKD by GFR and age, and the prevalence of micro- and macroalbuminuria by GFR and age. We prioritized matching our model outcomes to the prevalence of CKD by age and the cumulative incidence of end-stage renal disease. The calibrated parameters include diabetes incidence rates, microalbuminuria incidence rates, and the transition probability from microalbuminuria to macroalbuminuria. All model parameters were informed by systematic review, existing models, and NHANES. We used grid search and imposed a range constraint such that the calibrated parameters are varied within allowable ranges of ±30% of the initial parameter values.

Relevant Assumptions

The main assumption governing the chronic kidney disease component is that the risk of developing CKD and progressing to more severe CKD stages depends on the presence of risk factors including age, sex, race, diabetes, and hypertension. Additionally, worsening kidney functions such as low GFR and/or macroalbuminuria leads to an acceleration of disease worsening

Relevant Parameters

Parameters associated with the Chronic kidney disease component are listed in the Parameter Overview.

Dependent Outputs

- Prevalence of CKD
- Prevalence of micro- or macroalbuminuria among persons with CKD
- Incidence of end-stage renal disease
- End-stage renal disease mortality

References

1. A. Levin, P. E. Stevens. Summary of KDIGO 2012 CKD Guideline: behind the scenes, need for guidance, and a framework for moving forward. Kidney Int. 2014;85(1):49–61.
2. United States Renal Data System. 2023 USRDS Annual Data Report: Epidemiology of kidney disease in the United States [Internet]. 2023. Available from: https://adr.usrds.org/2023

Columbia University
Natural History
Component

COLUMBIA UNIVERSITY

Natural History Component

Summary

This document describes the natural history model including the progression from a cancer-free state to death from metastatic disease.

Overview

The natural history model of SCOUT simulates the development of undetectable low-grade or high-grade papillary tumors. These tumors may progress by increasing in grades, transition from undetectable to detectable or from detectable to detected state, and advancing in T stages, and eventually reaching metastatic disease. The disease progression follows nonhomogeneous Markov model with a monthly cycle and a lifetime horizon. SCOUT incorporates risk factors associated with risk of bladder cancer including sex, age, race, risk behavior of smoking, and chronic kidney disease (CKD) severity.

Details

SCOUT simulates the development and progression of bladder cancers with four main health states: disease-free, non-muscle invasive bladder cancers or NMIBC (Ta, Tis, T1), muscle invasive bladder cancers or MIBC (T2, T3, T4 excluding metastatic disease), and metastasis, using a monthly cycle. The model incorporates risk factors associated with the risk of bladder cancers including age, sex, race, smoking status, and CKD stage. At the beginning of the time horizon, SCOUT simulates a hypothetical cohort of the same sex, age, and race. Each person is assigned one of the three smoking statuses (Never, Former, Current), which remains static in the current version of SCOUT, and a CKD stage based on their glomerular filtration rate and albuminuria category (See Chronic Kidney Disease component for more details). SCOUT tracks individual change in CKD stage, which in turn influence the rates of bladder tumor development and the mortality rates. The natural history of bladder cancer component is initiated when the cohort reaches age 40, given the low prevalence of bladder cancer before this age.

SCOUT explicitly models three states—undetectable (tumor presence without symptoms), detectable (microscopic or macroscopic hematuria), and detected—for each of TaLG and TaHG-Tis combined in NMIBC. For MIBC, any T stages are assumed to be symptomatic and detectable. However, only a proportion of these tumors are detected according to the observed cancer incidence from SEER cancer registry. Any detected cancers are assumed to be treated according the NCCN guidelines. The treatment module is currently in development. The development and progression of bladder cancer in SCOUT follows a Markov model (Figure 1), where the transition probability at cycle t depends only on the health state at cycle t–1. To apply a Markov model, SCOUT follows the steps below:

1. A transition matrix is first established based on all transition probability inputs listed in the Parameter Overview.
2. The probability of remaining in the same health state is calculated as 1 minus the sum of probabilities of transitioning to other states.
3. At each cycle, the next health state is determined by sampling from a categorical distribution, using the probability distribution derived from the transition matrix.
4. The transition matrices are updated monthly to account for individual changes in various risk factors.

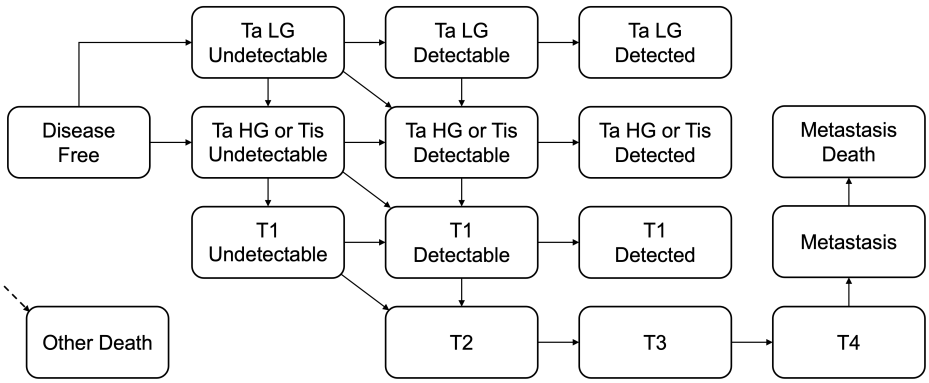

Figure 1. State-transition diagram depicting the progression of bladder cancer from a disease-free state to T stages among non-muscle and muscle invasive bladder cancers, metastasis, and death from metastasis or other death.

Persons who are initially disease-free may develop bladder tumor through one of the two pathways: 1) developing low-grade papillary bladder tumor or TaLG or 2) developing high-grade papillary bladder tumor or TaHG. For simplicity, TaHG and Tis are grouped into a combined state. At any cycle, persons with a bladder tumor may transition to more severe states including transitioning from undetectable to detectable state, from detectable to detected state, from low to high grade, increase in T stage, and may eventually reach metastasis. At any cycle, persons may die from one of the competing causes of death including CVD, non-CVD, or metastasis death (applied only to persons with metastasis). SCOUT tracks individual trajectories of age, smoking status, CKD stage, health state at cycle t and cycle t–1, death status, and causes of death.

To align with the observational bladder cancer incidence from SEER, we calibrated SCOUT for white men using incremental mixture approximate Bayesian computation algorithm [1] to the age- and stage-specific cancer incidence. The calibrated parameters include the probability of developing bladder tumor, the probability of transitioning from undetectable to detectable state, the probability of transitioning from detectable to detected state, the probability of transitioning from less severe to more severe T stages, and the proportion of cancer detected in MIBC.

Relevant Assumptions

The main assumption governing the natural history model is that all cancers must arise from either low-grade or high-grade papillary tumors. Among NMIBC, all tumors go from an undetectable state to a detectable state and reach a detected state if they are clinically diagnosed. MIBC is assumed to be symptomatic and detectable with a proportion assumed to be detected according to SEER observed incidence. Additionally, the risk for bladder cancer increases for those with older age, having severe CKD stages, or are smokers.

Relevant Parameters

Parameters associated with the Natural history component are listed in the Parameter Overview.

Dependent Outputs

- Age- and stage-specific cancer incidence
- Cancer stage at diagnosis
- Cancer mortality

References

1. Carolyn M. Rutter, Jonathan Ozik, Maria DeYoreo, Nicholson Collier. Microsimulation model calibration using incremental mixture approximate Bayesian computation. The Annals of Applied

Statistics. 2019;13(4):2189–2212, 24.

Key References

M. Afkarian, M. C. Sachs, B. Kestenbaum, I. B. Hirsch, K. R. Tuttle, J. Hinnmelfarb, et al. Kidney Disease and Increased Mortality Risk in Type 2 Diabetes. Journal of the American Society of Nephrology. 2013;24(2):302–308.

L. E. Boulware, B. G. Jaar, M. E. Tarver-Carr, F. L. Brancati, N. R. Powe. Screening for proteinuria in US adults: a cost-effectiveness analysis. JAMA. 2003;290(23):3101–14.

Emily R Brooks, Mutita Siriruchatanon, Vinay Prabhu, David M Charytan, William C Huang, Yu Chen, et al. Chronic kidney disease and risk of kidney or urothelial malignancy: systematic review and meta-analysis. Nephrology Dialysis Transplantation. 2023;

H. Calkins, Y. Shyr, H. Frumin, A. Schork, F. Morady. The value of the clinical history in the differentiation of syncope due to ventricular tachycardia, atrioventricular block, and neurocardiogenic syncope. Am J Med. 1995;98(4):365–73.

A. Christensson, C. Savage, D. D. Sjoberg, A. M. Cronin, M. F. O'Brien, W. Lowrance, et al. Association of cancer with moderately impaired renal function at baseline in a large, representative, population-based cohort followed for up to 30 years. Int J Cancer. 2013;133(6):1452–8.

N. D. Freedman, D. T. Silverman, A. R. Hollenbeck, A. Schatzkin, C. C. Abnet. Association between smoking and risk of bladder cancer among men and women. JAMA. 2011;306(7):737–45.

A. X. Garg, B. A. Kiberd, W. F. Clark, R. B. Haynes, C. M. Clase. Albuminuria and renal insufficiency prevalence guides population screening: results from the NHANES III. Kidney Int. 2002;61(6):2165–75.

A. S. Go, G. M. Chertow, D. Fan, C. E. McCulloch, C. Y. Hsu. Chronic kidney disease and the risks of death, cardiovascular events, and hospitalization. N Engl J Med. 2004;351(13):1296–305.

T. J. Hoerger, J. S. Wittenborn, J. E. Segel, N. R. Burrows, K. Imai, P. Eggers, et al. A health policy model of CKD: 1. Model construction, assumptions, and validation of health consequences. Am J Kidney Dis. 2010;55(3):452–62.

A. Levin, P. E. Stevens. Summary of KDIGO 2012 CKD Guideline: behind the scenes, need for guidance, and a framework for moving forward. Kidney Int. 2014;85(1):49–61.

Y. Lotan, K. Elias, R. S. Svatek, A. Bagrodia, G. Nuss, B. Moran, et al. Bladder cancer screening in a high risk asymptomatic population using a point of care urine based protein tumor marker. J Urol. 2009;182(1):52–7; discussion 58.

W. T. Lowrance, J. Ordonez, N. Udaltsova, P. Russo, A. S. Go. CKD and the risk of incident cancer. J Am Soc Nephrol. 2014;25(10):2327–34.

E. M. Messing, T. B. Young, V. B. Hunt, J. M. Wehbie, P. Rust. Urinary tract cancers found by homescreening with hematuria dipsticks in healthy men over 50 years of age. Cancer. 1989;64(11):2361–7.

E. M. Messing, T. B. Young, V. B. Hunt, E. B. Roecker, A. M. Vaillancourt, W. J. Hisgen, et al. Home screening for hematuria: results of a multiclinic study. J Urol. 1992;148(2 Pt 1):289–92.

E. M. Messing, T. B. Young, V. B. Hunt, K. W. Gilchrist, M. A. Newton, L. L. Bram, et al. Comparison of bladder cancer outcome in men undergoing hematuria home screening versus those with standard clinical presentations. Urology. 1995;45(3):387–96; discussion 396-7.

E. M. Messing, T. B. Young, V. B. Hunt, M. A. Newton, L. L. Bram, A. Vaillancourt, et al. Hematuria home screening: repeat testing results. J Urol. 1995;154(1):57–61.

S. D. Navaneethan, J. D. Schold, S. Arrigain, S. E. Jolly, Jr. Nally J. V. Cause-Specific Deaths in Non-Dialysis-Dependent CKD. J Am Soc Nephrol. 2015;26(10):2512–20.

Carolyn M. Rutter, Jonathan Ozik, Maria DeYoreo, Nicholson Collier. Microsimulation model calibration using incremental mixture approximate Bayesian computation. The Annals of Applied Statistics. 2019;13(4):2189–2212, 24.

R. L. Siegel, K. D. Miller, N. S. Wagle, A. Jemal. Cancer statistics, 2023. CA Cancer Journal for Clinicians. 2023;73(1):17–48.

United States Renal Data System. 2023 USRDS Annual Data Report: Epidemiology of kidney disease in the United States [Internet]. 2023. Available from: https://adr.usrds.org/2023

B. O. Yarnoff, T. J. Hoerger, S. S. Shrestha, S. K. Simpson, N. R. Burrows, A. H. Anderson, et al. Modeling the impact of obesity on the lifetime risk of chronic kidney disease in the United States using updated estimates of GFR progression from the CRIC study. PLoS One. 2018;13(10):e0205530.